Isolation and structural characterization of a subset of yeast (*Saccharomyces cerevisiae*) peroxisomal proteins

by

Munmun Santi Nandi

A Thesis submitted to the Faculty of Graduate Studies of

The University of Manitoba

in the partial fulfilment of the requirements of the degree of

MASTER OF SCIENCE

Department of Microbiology

University of Manitoba

Winnipeg

ABSTRACT

Peroxisomes are virtually found in all eukaryotic cells, but unlike mitochondria and chloroplasts, they do not contain DNA or a protein secretory apparatus. Therefore, all of their proteins must be imported by a process called peroxisomal biogenesis. This requires a group of protein factors referred to as peroxins which are encoded by the *pex* genes. Currently, there are approximately thirty-two known peroxisomal proteins. Among all the peroxisomal proteins, two enzymes namely GPD1, LYS1 and a peroxin, PEX7 were selected for the research. GPD1 is a NAD^+ -dependent glycerol 3-phosphate dehydrogenase1 that catalyzes the conversion of dihydroxyacetone phosphate (DHAP) to glycerol 3-phosphate which is crucial for growth under osmotic stress. Its purification was achieved using ion exchange chromatography and the pure protein was crystallized for structure determination. Diffraction data sets were obtained to a resolution of 2.2 Å which were used to solve the C-terminal portion of the structure. Unfortunately, the N-terminal portion remained disordered. LYS1 is the terminal enzyme of α-aminoadipate pathway and catalyzes the reversible NAD-dependent oxidative cleavage of saccharopine to yield L-lysine and α-ketoglutarate. The purification of LYS1 was carried out using affinity chromatography. Another protein, PEX7 is responsible for peroxisome biogenesis by importing newly synthesized proteins bearing PTS2 (peroxisome targeting signal sequence2) into peroxisomes. PEX7 presented the greatest challenge among the three proteins at both the expression stage and the purification stage. Its soluble fraction was purified using ion exchange and affinity chromatographies, although the final yield was too low for crystallization trials. A much large proportion of the protein was found in the insoluble cell debris and attempts were made to purify this fraction after denaturation. An alternative, protocol involving the formation of a GPD1-PEX7 complex proved to be effective route to co-purification of the two proteins and crystallization trials are proceeding. Having known the structures of peroxisomal proteins, it would be helpful for studying the development and maintenance of the organelle related to its metabolic diseases in the eukaryotic cells.

ACKNOWLEDGEMENTS

First and foremost, I would like to thank my supervisor Dr. Peter C. Loewen for giving me the opportunity to work in his lab and for the immense guidance and continuous support for over two and half years. His patience and devotion to his research will be an inspiration for me throughout my future career. I would also like to thank the members of my advisory committee, Dr. Teresa de Kievit, Dr. Deborah Court, and Dr. Michelle Piercey-Normore for their thoughtfulness and many important suggestions throughout the course of this work. I am very grateful to Jack Switala, Jacylyn Villanueva and everybody in the lab, Vikash Jha, Ben Wiseman, Tuhin Guha and Jason Chan for all their suggestions, technical help and more importantly their friendship. Also I would like to thank our collaborators, Dr. Ignacio Fita and Dr. Xavier Carpena in Barcelona for the crystallography. I sincerely thank Terry James and Veronica Larmour for guidance regarding the FPLC machine and giving me a constant encouragement to pursue the protein purification stage. Next, I would like to thank all the faculty, staff and students of the Department of Microbiology for their kindness and assistance over the years. Finally, I would like to thank God to whom I believe and my parents without whom it could have never been possible.

TABLE OF CONTENTS

	Page
ABSTRACT	ii
ACKNOWLEDGEMENTS	iii
TABLE OF CONTENTS	iv
LIST OF FIGURES	vii
LIST OF TABLES	ix
LIST OF ABBREVIATIONS	x
1. INTRODUCTION	**13**
1.1. Peroxisome	**13**
1.1.1. Overview of the peroxisome: Brief description on structure and function	13
1.1.2. Biogenesis of peroxisome	16
1.1.2.1. Models of peroxisome biogenesis and multiplication	16
1.2. Biogenesis of Peroxisome in yeast	**18**
1.2.1. Peroxisomal Targeting Signal Sequences (PTS)	18
1.2.2. Import of matrix proteins	20
i. Protein recognition by receptor	20
ii. Docking of the receptor-protein complex on the peroxisomal membrane	21
iii. Membrane translocation of the receptor-protein complex	22
iv. Receptor recycling	23
1.3. Peroxisomal disorders	**28**
1.4. Peroxisomal proteins selected for study	**30**
1.4.1. Glycerol-3-phosphate dehydogenase1 (GPD1)	30
1.4.2. Saccharopine dehydrogenase1 (LYS1)	34
1.4.3. Peroxin7 (PEX7)	37
1.5. Objective of thesis	**38**

2. MATERIALS AND METHODS 39

2.1. Biochemical and common reagents 39

2.2. *Escherichia coli* strains and plasmids 39

2.3. Culture media and storage media 41

2.4. Antibiotic concentrations in the growth media 41

2.5. DNA manipulation 41

2.5.1. DNA isolation and purification 41

2.5.2. PCR amplification 42

2.5.3. Agarose gel electrophoresis 43

2.5.4. Restriction endonuclease digestion of DNA 43

2.5.5. Ligation 44

2.5.6. Transformation 44

2.5.7. DNA sequencing 45

2.5.8. Cloning in pET28b+ vector 46

2.6. Recombinant protein expression 46

2.7. Recombinant protein purification 47

2.7.1. Purification of GPD1 48

2.7.2. Purification of LYS1 49

2.7.3. Purification of PEX7 51

2.8. *In vitro* binding assay 52

2.9. Protein analysis 53

2.9.1. Determination of protein concentration 53

2.9.2. Sodium dodecyl sulfate-polyacrylamide gel electrophoresis (SDS-PAGE) 53

2.10. Enzyme activity 54

2.10.1. Enzyme activity of GPD1 54

2.10.2. Enzyme activity of LYS1 54

2.11. GPD1 crystallization and structure determination 54

3. RESULTS **56**

3.1. Glycerol-3-phosphate dehydrogenase1 56

3.1.1. Construction of pET28b-GPD1 56

3.1.2. Protein expression 56

3.1.3. Protein purification 60

3.1.4. Enzyme activity of GPD1 62

3.1.5. Crystallization and structure determination 62

3.2. Saccharopine dehydrogenase1 **65**

3.2.1. Construction of pET28b-LYS1 65

3.2.2. Protein expression 66

3.2.3. Protein purification 68

3.2.4. Enzyme activity of LYS1 73

3.3. Peroxin7 **73**

3.3.1. Construction of pET28b-PEX7 73

3.3.2. Protein expression 73

3.3.3. Protein purification 77

3.4. *In vitro* binding assay **83**

4. Conclusion **84**

4.1. Expression, purification and crystallization of a subset of *Saccharomyces cerevisiae* peroxisomal proteins 84

4.1.1. GPD1 84

4.1.2. LYS1 85

4.1.3. PEX7 85

4.2. Future directions **87**

5. REFERENCES **88**

LIST OF FIGURES

Page

Figure 1-1: Electron micrograph of yeast peroxisome 13

Figure 1-2: Overview of peroxisomal functions in yeast 15

Figure 1-3: Model of the life cycle of peroxisomes 17

Figure 1-4: Role of PTS1 and PTS2 in import of matrix proteins into peroxisomes 19

Figure 1-5: The import of peroxisomal matrix proteins 25

Figure 1-6: Catalytic conversion of dihydroxyacetone phosphate to glycerol-3-phosphate 32

Figure 1-7: Cartoon representation of the structure of human GPD1 33

Figure 1-8: Catalytic conversion of saccharopine to lysine and α-ketoglutarate 35

Figure 1-9: Cartoon representation of the structure of saccharopine dehydrogenase from *S. cerevisiae* 36

Figure 3-1: Construction of pKS-GPD1 and pET28b-GPD1 57

Figure 3-2: Small scale expression trials of GPD1 58

Figure 3-3: Fractionation of GPD1 by ammonium sulfate 59

Figure 3-4: Purification of GPD1 on DEAE cellulose 61

Figure 3-5: Crystals of GPD1 observed and used for data collection 62

Figure 3-6: Cartoon representation of the crystal structure of yeast GPD1 64

Figure 3-7: Construction of LYS1-pET28b 65

Figure 3-8: Small scale expression trials of LYS1 66

Figure 3-9: Fractionation of LYS1 by ammonium sulfate 67

Figure 3-10: Purification of LYS1 on DEAE cellulose 69

Figure 3-11: Purification of LYS1 on 1 mL HiTrap nickel column 71

Figure 3-12: Purification of LYS1 on Ni-NTA Superflow resin 72

Figure 3-13: Construction of PEX7-pKS and PEX7-pET28b 74

Figure 3-14: Small scale expression trials of PEX7 75

Figure 3-15: Fractionation of PEX7 by ammonium sulfate 76

Figure 3-16: Purification of PEX7 on Superose 12 followed by nickel column 78

Figure 3-17: Purification of PEX7 on DEAE cellulose followed by nickel column 80

Figure 3-18: Protein expression in Rosetta (DE3) 81

Figure 3-19: Solubilization of cell debris and purification on Ni-NTA Superflow resin 82

Figure 3-20: *In vitro* binding assay on Ni-NTA Superflow resin 83

LIST OF TABLES

Page

Table 1-1: Proteins (Peroxins) involved in the biogenesis of peroxisomes in yeast 26

Table 2-1: Genotype and sources of *Escherichia coli* strains and plasmids used in this study 40

Table 2-2: Oligonucleotide primers used for PCR amplification 42

Table 2-3: Protein expression plasmids used over the course of the study 46

Table 3-1: Data collection and refinement statistics for GPD1 63

LIST OF ABBREVIATIONS

A_{280}	Absorbance at 280 nanometres
Å	Angstrom
Amp	Ampicillin
AAA	ATP Associated with other cellular Activities
ATP	Adenosine Tri-Phosphate
α-KG	Alpha-ketoglutarate
bp(s)	Base pair(s)
^{o}C	degree Celsius
CBB	Coomassie Brilliant Blue
CV	Column volume
Da	Dalton
DEAE	Diethylaminoethyl
DHAP	Dihydroxyacetone phosphate
DMSO	Dimethylsulphoxide
DNA	De-oxyribonucleic acid
DTT	Dithiothreitol
EDTA	Ethylenediaminetetraacetic Acid
E.coli	*Escherichia coli*
FPLC	Fast protein liquid chromatography
g	Gram
GTPase	Guanosine Triphosphatase
His	Histidine
IPTG	Isopropyl β-D-thiogalactopyranoside
Kan	Kanamycin
kDa	kilo Dalton
kbp(s)	kilo base pair(s)
L	Litre
LB	Luria-Bertani
µL	Microlitre
µM	Micromolar

M	Molar
mAu	milli-Absorption Units
mg	Milligram
mL	Millilitre
mM	Millimolar
min	Minute
MW	Molecular weight
MWCO	Molecular weight cut-off
NAD	Nicotinamide adenine dinucleotide
ng	Nanogram
nm	Nanometre
ON	Overnight
OD_{600}	Optical density at 600 nanometres
ORF	Open reading frame
PAGE	Polyacrylamide gel electrophoresis
PBS	Phosphate Buffered Saline
PCR	Polymerase chain reaction
PDB	Protein data bank
PEX	Peroxin
pM	Picomolar
psi	Pounds per square inch
PTS	Peroxisomal targeting sequence
RNA	Ribonucleic acid
rpm	Revolutions per minute
SDS-PAGE	Sodium Dodecyl-phosphate Poly-Acrylamide Gel Electrophoresis
TAE	Tris-Acetate EDTA buffer
TPR	Tetratricopeptide repeat
Tris	Tris (hydroxymethyl) aminomethane
U	Units
V	Volts
w/v	Weight per unit volume

Anyone who has never made a mistake has never tried anything new.

- Albert Einstein

1. INTRODUCTION

1.1 Peroxisome

1.1.1 Overview of the peroxisome: Brief description on structure and function

Peroxisomes are compartmentalized microbodies that are bound by a single membrane and are present in most eukaryotic cells and organisms (Cavalier-Smith, 1987). The organelles were first discovered by the Belgian scientist Christian de Duve in the year 1965 (de Duve, 1969). The protein content of peroxisomes varies across species, but the presence of proteins common to many species has been used to suggest an Endosymbiotic origin; that means, peroxisomes evolved from bacteria that invaded larger cells as parasites and evolved into a symbiotic relationship gradually (Gabaldon, 2010). They are generally spherical of variable size and with a granular or crystalline-like interior (Figure 1-1).

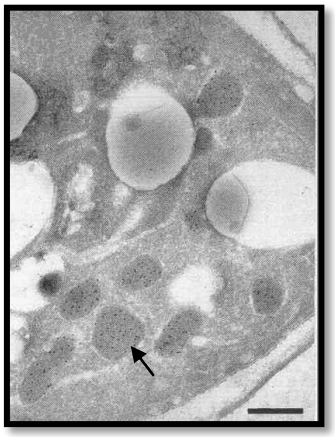

Figure 1-1: Electron micrograph of yeast peroxisome; Electron micrograph of glutaraldehyde-fixed cell stained with uranylacetate. The arrow indicates a peroxisome. The bar indicates 0.5 micrometers.

Peroxisomes fulfill essential metabolic functions in lipid metabolism, both catabolic (oxidation of very-long chain fatty acids) (Figure 1-2) and anabolic (synthesis of plasmalogens and bile acids). Moreover, peroxisomes have key roles in free radical detoxification, differentiation, development and morphogenesis (Alberts et al., 2002). In particular, their role in the elimination of hydrogen peroxide by catalase is well known (del Rio et al., 1992).

The oxidative degradation of fatty acids via beta-oxidation is a key process carried out in the peroxisomes. The alkyl chains of fatty acids are shortened sequentially by blocks of two carbon atoms at a time, thereby converting the fatty acids to acetyl CoA. The acetyl CoA is then exported from the peroxisomes to the cytosol for reuse in biosynthetic reactions (Kunau et al., 1995) (Figure 1-2). In mammalian cells, β oxidation occurs in both mitochondria and peroxisomes whereas, in fungi (e.g. *Neurospora crassa*, yeast) and plant cells, this essential reaction occurs exclusively in peroxisomes (Hiltunen et al., 2006). Other peroxisomal processes include lysine biosynthesis, the glyoxylate shunt and the degradation of methanol and amino-acids (Wanders and Waterham, 2006) (Figure 1-2).

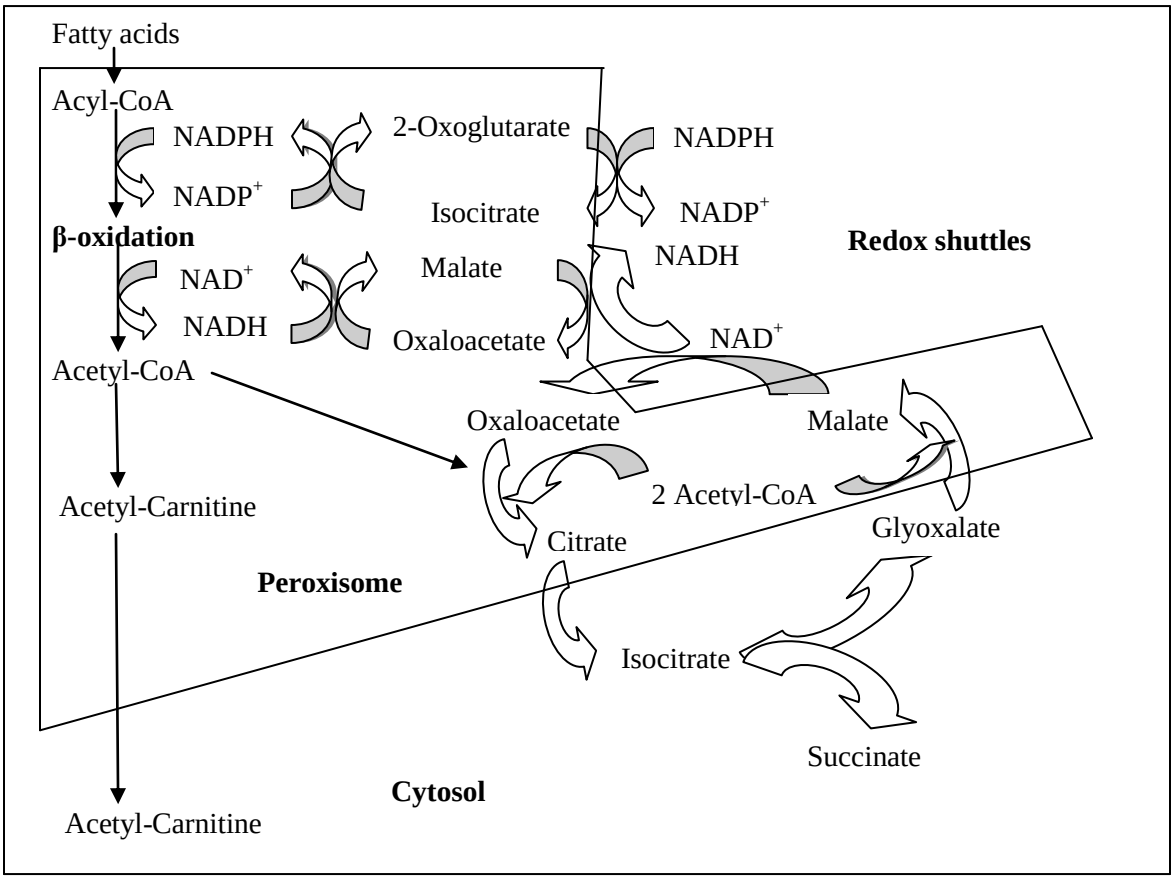

Figure 1-2: Overview of peroxisomal functions in yeast; In yeasts, peroxisomes contain several oxidases which oxidize specific carbon and nitrogen sources. The larger organelles develop from small peroxisomes present in glucose grown cells as a result of rapid synthesis of peroxisomal enzymes, such as catalase and alcohol dehydrogenase. The peroxisomes are the primary site of fatty acid degradation in yeast. Acetyl-CoA, NADH and NADPH are produced in peroxisomes (*Zinser and Daum, 1995)*.

1.1.2 Biogenesis of peroxisomes

Peroxisomes have relatively short life spans of just one to two days and this gives rise to a constant process of replacement. Organelles such as chloroplasts and mitochondria contain a rudimentary genome which reveals their bacterial ancestry; but peroxisomes contain no DNA or ribosomes and therefore have no means of protein production. Therefore, all peroxisomal proteins must be imported across the membrane giving rise to the process of peroxisomal biogenesis involving self assembly (Purdue and Lazarow, 2001).

1.1.2.1 Models of peroxisome biogenesis and multiplication

The developmental origin of the membrane and the different times in the life cycle of the peroxisome at which the various peroxisomal membrane proteins are recruited remains controversial (Tabak et al., 2003). The growth and division of peroxisomes involves the post-translational import of peroxisomal matrix and membrane proteins after their synthesis in the cytosol (Lazarow 2003). It was generally assumed that the membrane phospholipids were transported to the peroxisomal membrane involving a poorly understood and characterized mechanism (Titorenko and Rachubinski, 2001), but this has recently been questioned. For example, the contribution of de novo formation from the ER was recently analyzed against growth and fission of existing peroxisomes leading to the conclusion that peroxisome formation more likely involves an alternative system that has yet to be characterized (Figure 1-3) (Schrader and Fahimi, 2006).

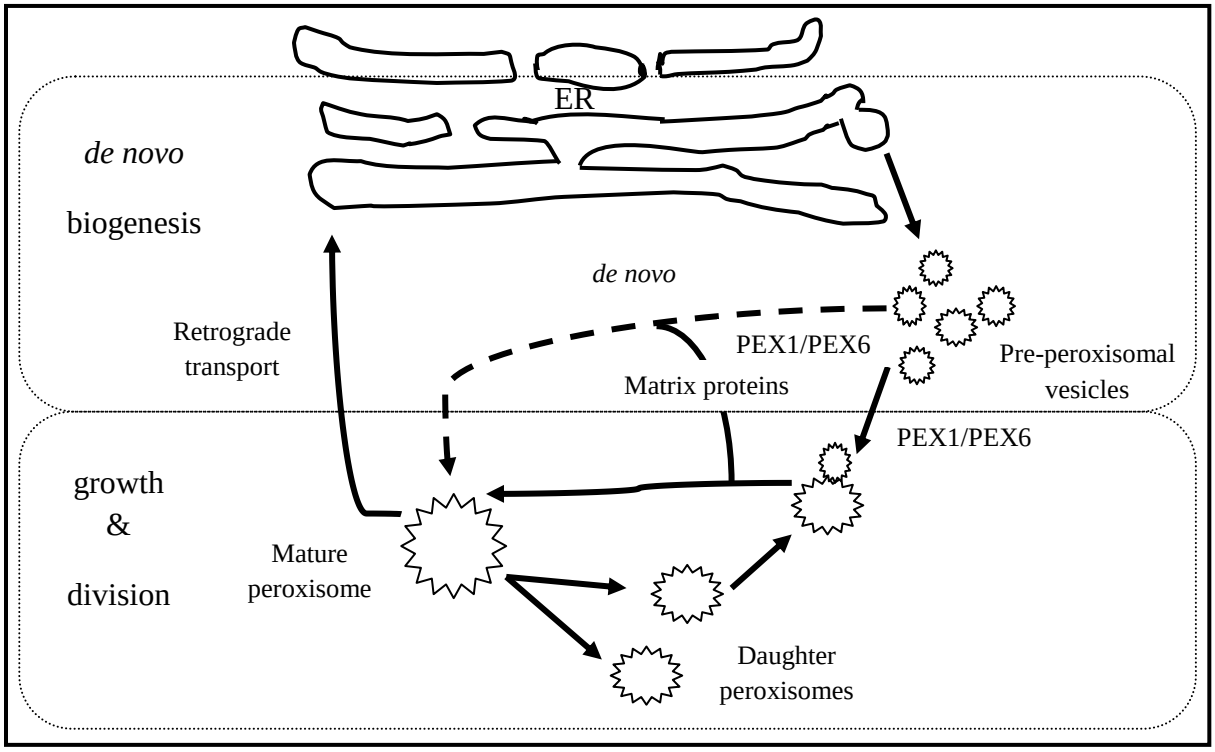

Figure 1-3: Model of the life cycle of peroxisomes; Peroxisomes proliferate and multiply by growth and division involving the post-translational import of new matrix proteins after their synthesis in the cytosol on free polyribosomes. In yeast and mammalian cells, *de novo* synthesis from the ER or the formation of pre-peroxisomal vesicles from a specialized compartment of the ER has been reported. The new vesicles then develop into mature peroxisomes via a multistep pathway involving different populations of pre-peroxisomes. Fusions between pre-peroxisomal vesicles and/or with existing peroxisomes are mediated in an ATP-dependent process by peroxisomal proteins (PEX1 and PEX6).

1.2 Biogenesis of peroxisomes in yeast

The biogenesis of peroxisomes in yeast requires a group of protein factors referred to as peroxins which are encoded by the *pex* genes (Eckert and Erdmann 2003). Altogether, 32 peroxins from different organisms have been identified as being involved in different aspects of peroxisome biogenesis (Table 1-1). They are all synthesized on free ribosomes in the cytoplasm and imported posttranslationally into the peroxisome via processes that involve Peroxisome Targeting Signal sequences (PTS) (Brown and Baker, 2003).

1.2.1 Peroxisome Targeting Signal Sequences (PTS)

Two types of peroxisomal targeting signal sequences (PTSs), namely PTS1 and PTS2 are responsible for directing newly synthesized proteins into the peroxisome (Figure 1-4). Most matrix proteins contain a PTS1 signal which consists of the C-terminal conserved tripeptide, S-K-L or its variant (S/A/C)-(K/R/H)-L (Gould et al., 1989). In fact, more recent studies have suggested more variability in the signal motif, including both length and sequence, and that the signal may vary between species (Neuberger et al., 2003). The current view is that the final 12 C-terminal residues influence PTS1 protein binding to PTS1 protein receptor. A small number of matrix proteins contain an N-terminal PTS2 targeting signal comprised of the consensus nonapeptide sequence (R/K)-(L/I/V)-X5-(H/Q)-(L/A/F) within the first 20 residues, although this varies between species (Petriv et al., 2004).

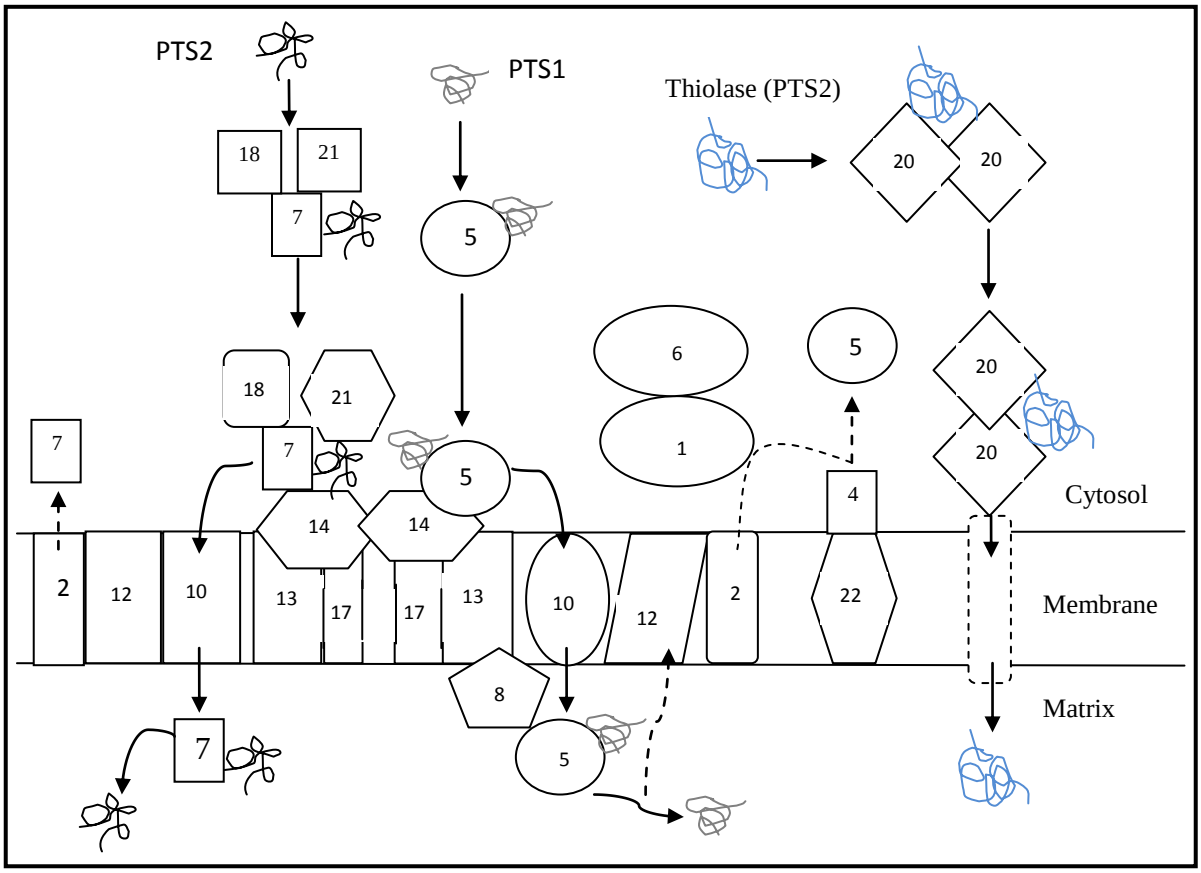

Figure1-4: Role of PTS1 and PTS2 in import of matrix proteins into peroxisomes; The peroxisomal targeting signals of matrix proteins, PTS1 (grey) and PTS2 (black), are recognized in the cytosol by their cognate receptors PEX5 and PEX7, respectively. The cytosolic peroxins PEX18 and PEX21 function in the delivery of PTS2-cargoloaded PEX7 to the outer face of the peroxisomal membrane. After their interaction with the docking subcomplex composed of PEX13, PEX14 and PEX17, PEX5 and PEX7 are transferred to the components of the translocation machinery, including PEX2, PEX10 and PEX12. PEX1, PEX2, PEX4, PEX6, PEX8 and PEX22 are involved in recycling the PTS1 receptor (dotted lines) to the cytosol. The cytosolic chaperone PEX20 assists the oligomerization of the PTS2-containing protein thiolase (blue) and maintains its import-competent oligomeric state.

1.2.2 Import of matrix proteins

The import of peroxisomal matrix proteins can be divided into four stages: protein recognition by a receptor, docking of receptor-protein complex on the peroxisomal membrane, membrane translocation of the receptor-protein complex and receptor recycling.

i. Protein recognition by receptor

The first step in peroxisomal protein import involves the interaction of the targeting sequence with a receptor. PTSs are first recognized in the cytosol by either the PTS1 receptor, PEX5, or the PTS2 receptor, PEX7 (Figure 1-5), which appear to cycle between the cytosol and the peroxisome (Dodt and Gould, 1996; Elgersma et al., 1998). PTS1 interactions with PEX5 have been mapped to the seven tetratricopeptide repeats (TPRs) located in the carboxy portion of PEX5. TPRs are degenerate 34 amino acid repeat units present on proteins involved in diverse cellular functions. The crystal structure of TPR domains reveals a helix-turn-helix motif with interacting anti-parallel α-helices. Both the inner and outer face of the super helix accommodates protein-protein interactions which may indicate the simultaneous interaction of PEX5-TPR interface with multiple proteins (Gatto et al., 2000; Maynard et al., 2004). The binding of PEX7 to peroxisomal matrix proteins depends on PTS2 (Rehling et al., 1996). All PEX7 protein homologs have WD motifs (i.e., tryptophan-aspartic acid repeat sequence approximately 31-40 amino acids long) which coordinate the simultaneous interaction of multiple proteins (Smith et al., 1999). Moreover, in lower eukaryotes like yeast, PTS2 targeting requires accessory proteins, PEX18 and PEX21 (Purdue et al., 1998). Thus, both PEX5 and PEX7, after recognition of their respective PTSs, are believed to induce conformational alterations in

the C- (PTS1) and N-terminal (PTS2) regions of the bound proteins to promote interactions with docking partners on the peroxisomal membrane (Azevedo et al., 2004; Gouveia et al., 2003).

ii. Docking of the receptor-protein complex on the peroxisomal membrane

The docking complex, present on the peroxisomal membrane has several binding sites which are thought to provide a template for sequential interaction of receptor-protein complexes with the docking site and subsequent recycling of the receptors (Reguenga et al., 2001). The peroxins which are responsible for providing the contact platform include an integral membrane protein, PEX13 and the peripheral membrane proteins, PEX14 and PEX17 (Elgersma et al., 1996; Girzalsky et al., 1999; Snyder et al., 1999) (Figure 1-5). Based on X-ray crystallography and NMR spectroscopy, PEX13 has a C-terminal, cytosolically oriented SH3 or Src Homology3 domain which is a small conserved sequence of about 60 amino acid residues that interacts with proline-rich peptides and is known to be involved in protein-protein interactions. This domain mediates the binding of PEX5 with PEX14, a type II SH3 ligand (Pires et al., 2003). The localization of the N-terminal part of PEX14 has not been determined, but it is most likely in the cytoplasm where it is responsible for PEX5 binding. *In vitro* studies with mammalian, plant and trypanosomatid PEX14 have shown that WXXXF/Y pentapeptide motifs in PEX5 are mutually-independent high-affinity binding sites for PEX14 (Saidowsky et al., 2001). Moreover, each of the WXXXF/Y motifs involved in binding is part of an amphipathic α-helix allowing the direct interaction between its hydrophobic residues and those of PEX14 (Choe et al., 2003). Additionally, the strength of the PEX5-PEX14 interaction is affected by the formation of a PTS1 peptide-PEX5 complex (Jardim et al., 2002). PEX14

was also shown to bind to PEX13 and PEX17, although the latter does not appear to be required for docking of the receptor to the peroxisomal membrane. In the PTS2 protein-import process, PEX7 binds directly to the docking complex, and the PEX7 interaction domain of PEX13 was mapped to its N-terminal 100 residues, to which also PEX18 and PEX21 bind (Stein et al., 2002).

iii. Membrane translocation of the receptor-protein complex

The core components of the system involved in translocation of the receptor-cargo complex following docking on the membrane are PEX2, PEX10 and PEX12 (Okumoto et al., 2000) (Figure 1-5). PEX10 and PEX12 are grouped together with PEX2 in a separate translocation subcomplex, distinct from the docking subcomplex where they show a strong association with PEX5 and PEX14. PEX2, PEX10 and PEX12 are integral peroxisomal membrane proteins with C_3HC_4 (RING) finger domains exposed to the cytosol. The two peroxins of the ring domains, PEX10 and PEX12, are responsible for interacting with each other as well as with PEX5. Moreover, *in vitro* studies have shown the interaction of PEX10 with PEX2 which is thought to act downstream of PEX10 and PEX12 (Collins et al., 2000). The complex of PEX2, PEX10 and PEX12 is involved in both PTS1 and PTS2 protein import.

The interaction of the docking complex with the RING complex requires intraperoxisomal PEX8 which is involved in both PTS1 and PTS2 import pathways. It has been proposed that PEX8 is responsible for the formation of a large, transient peroxisomal import complex which appears to be an essential coordinator of the docking subcomplex and the translocation subcomplex of the RING finger proteins (Agne et al., 2003). Significantly, because the docking and translocation steps do not require ATP

hydrolysis, it is likely that strong protein-protein interactions between PEX5 and other components of the system, such as PEX14, are the driving force behind translocation (Azevedo et al., 2004; Oliveira 2003).

iv. Receptor recycling

Proteins are imported in their folded and even oligomeric form into peroxisomes, glyoxysomes and glycosomes, and a "simple shuttle" model was initially envisioned for the process. The proteins were first bound by receptors in the cytosol, followed by docking on the membrane for transport of the protein into the peroxisome. More recently an "extended shuttle" model has been proposed in which the receptor-protein complexes are transported into the peroxisome followed by release of the protein and transport of the receptor back to the cytosol. This was based on the observation that PEX5 shuttles in and out of the matrix of mammalian peroxisomes (Dammai and Subramani, 2001). It was also shown that the N-terminus of mammalian PEX5 is required for redirecting the peroxin back to the cytosol (Costa-Rodrigues et al., 2004).

Two peroxins which have been implicated in receptor recycling are the membrane associated proteins PEX1 and PEX6 (Figure 1-5). They belong to a family of proteins with ATPase-associated activity (AAA) and interact with one another in an ATP-dependent manner. They act downstream of the docking and translocation steps and are part of the translocation machinery (Collins et al., 2000).

Another peroxisomal membrane protein, PEX26, associates with PEX1 and PEX6 in CHO cells (Matsumoto et al., 2003), as does PEX15 in yeast (Birschmann et al., 2003). PEX15 binds to PEX6 with most of its sequence facing the cytosol and its two AAA cassettes have opposite effects on the PEX6-PEX15 interaction (Moyersoen et al., 2005).

This is consistent with the cycle of binding and release being dependent on ATP hydrolysis catalyzed by these cassettes.

PEX5 undergoes monoubiquitination at cysteine 11, an unusual type of ubiquitination (Carvalho et al., 2007), catalyzed by PEX4, a specialized ubiquitin-conjugating enzyme in yeast (Williams et al., 2007) before being recycled back to the cytosol. Eventually, through an energy-dependent process by the action of PEX1 and PEX6, which are anchored to the peroxisomal membrane by PEX26, ubiquitinated PEX5 is returned to the cytosol available for further transport (Platta et al., 2005). Thus, PEX5 is once again available for further cycles of protein transport.

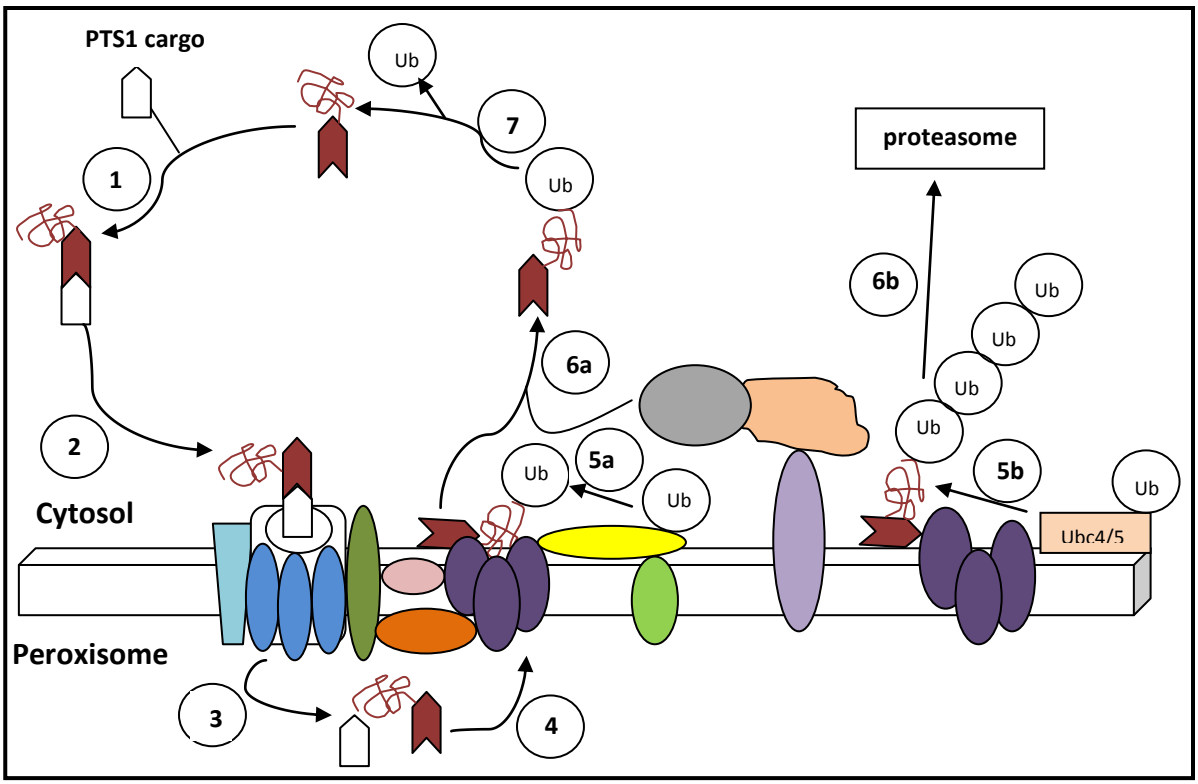

Figure1-5: The import of peroxisomal matrix proteins; The transport process can be divided into 7 steps (numbers in opened black circles). Coloured shapes indicate corresponding PEX proteins [brown-PEX5; aqua-PEX17; dark blue-PEX14; dark green-PEX13; pink-PEX3; orange-PEX8; purple-PEX12 (left), PEX10 (middle), PEX2 (right); yellow-PEX4; light green-PEX22; mauve-PEX15; light orange-PEX6; grey-PEX1]. (1) Receptor–cargo interaction in the cytosol (PTS2 pathway is not depicted). (2) Receptor–cargo docking at the peroxisomal membrane with the docking subcomplex, inducing the assembly of the translocon. (3) Translocation of the receptor–cargo complex across the membrane followed by the dissociation of the receptor–cargo complex; i.e., cargo release. (4) Export of cargo-free receptors from the peroxisome matrix to the membrane. (5a) Mono-ubiquitination of the receptor on a cysteine (for receptor recycling) or (5b) poly-ubiquitination of the receptor on a lysine by Ubc4/5 (for degradation by the RADAR pathway). (6a) Receptor recycling from the peroxisome membrane back to the cytosol, or (6b) degradation of a receptor that is blocked from recycling via the RADAR pathway involving the proteasome. (7) De-ubiquitination of the receptor before the next round of import (*Ma et al., 2011).*

Table 1-1: Proteins (Peroxins) involved in the biogenesis of peroxisomes in yeast

Peroxin	Localization	Proposed Function
PEX1	cytosol/membrane	Matrix protein import, export of PEX5
PEX2	membrane	Matrix protein import, translocation
PEX3	membrane	Membrane biogenesis, PMP import
PEX4	cytosol/membrane	Matrix protein import, PEX5 ubiquitination
PEX5	cytosol/membrane	Matrix protein import, PTS1 receptor
PEX6	cytosol/membrane	Matrix protein import, export of PEX5
PEX7	cytosol/membrane	Matrix protein import, PTS2 receptor
PEX8	matrix/membrane	Matrix protein import
PEX10	membrane	Matrix protein import, translocation
PEX11	membrane	Division and proliferation
PEX12	membrane	Matrix protein import, translocation
PEX13	membrane	Matrix protein import, docking
PEX14	membrane	Matrix protein import, docking
PEX15	membrane	Matrix protein import, PEX1/PEX6 anchor
PEX17	membrane	Matrix protein import, docking
PEX18	cytosol/membrane	Matrix protein import, PTS2 import
PEX19	cytosol/membrane	Membrane biogenesis, PMP import
PEX20	cytosol/membrane	Matrix protein import, PTS2 import

Table 1-1: continued

Peroxin	Localization	Proposed Function
PEX21	cytosol/membrane	Matrix protein import, PTS2 import
PEX22	membrane	Matrix protein import, PEX4 anchor
PEX23	membrane	Proliferation
PEX24	membrane	Proliferation
PEX25	membrane	Proliferation
PEX26	membrane	Matrix protein import, PEX1/PEX6 anchor
PEX27	membrane	Proliferation
PEX28	membrane	Proliferation (PEX24 ortholog)
PEX29	membrane	Proliferation
PEX30	membrane	Proliferation (PEX23 ortholog)
PEX31	membrane	Proliferation
PEX32	membrane	Proliferation

1.3 Peroxisomal disorders

Peroxisomal disorders are a group of congenital diseases in humans, characterized by the absence of normal peroxisomes in the cells of the body (Wanders et al., 1996). Most peroxisomal disorders cause severe neurological dysfunction due to central nervous system malformations, myelin abnormalities, and neuronal degeneration. Non-neurological manifestations include dysmorphic features, liver dysfunction and skeletal abnormalities (Powers and Moser, 1998). The key biochemical abnormalities of peroxisomal disorders are elevation of very long chain fatty acids and decreased red blood cell plasmalogens (Gould et al., 2001).

The biochemical classification has been customary since the early 1980s, when peroxisomal disorders were first being recognized and described. Since then, around 25 peroxisomal disorders have been identified, with a few more suspected or under investigation (Steinberg et al., 2006). These peroxisomal disorders can be categorized into two major groups: peroxisomal biogenesis disorders and single peroxisomal enzyme deficiencies.

The disorders caused by a failure to form intact, normal peroxisomes, resulting in multiple metabolic abnormalities, are referred to as peroxisome biogenesis disorders (PBD). PBDs are diseases in which the entire process of peroxisomal assembly has malfunctioned, and nearly all normal peroxisomal functions are either absent or deficient (Braverman et al., 1995). Consequently, either the peroxisomes fail to form in sufficient numbers, or else "ghost peroxisomes" are formed, having somewhat the appearance of the real peroxisome but lacking the matrix enzymes necessary to function (Gould et al., 2001). PBDs are caused by mutations of PEX genes that are involved in the biogenesis

and function of peroxisomes (Dimitri, 2010). For example, mutations in PEX7 normally cause Rhizomelic Chondrodysplasia Punctata (RCDP) type 1, a severe peroxisomal biogenesis disorder (Brink et al., 2003). Cultured fibroblasts from patients with RCDP are deficient for the PTS2 receptor protein, PEX7, and are unable to import the PTS2 reporter in the assay (Legakis et al., 2001) whereas expression of PEX7 in RCDP fibroblasts rescues the PTS2 protein import deficiency. Moreover, C-terminal truncation of PEX7 cosegregates with the disease (Motley et al., 1997). RCDP is characterized by certain skeletal abnormalities from which it derives its name, a dwarfism marked by a disproportionate shortening of the upper limbs (rhizomelia), and abnormalities in the formation of cartilage (chondrodysplasia punctata, specifically an abnormal calcification of cartilage) (Talwar and Swaiman, 1987).

In single peroxisomal enzyme deficiencies, peroxisomes are intact and functioning, except that there is a defect in just one enzymatic process, resulting in just one primary biochemical abnormality. These are caused by mutations of genes encoding specific peroxisomal enzymes and the loss of a single enzymatic function is sufficient to cause a disease which is as severe as the PBD (Steinberg et al., 2006). GPD1 and LYS1 provide two such examples.

i. GPD1 in yeast is a key enzyme for the synthesis of glycerol which is essential for cell growth during periods of reduced water availability (Albertyn et al., 1994). This is evident in GPD1 deletion mutants which produce very little glycerol and are sensitive to osmotic stress.

ii. LYS1 catalyzes the reversible conversion of saccharopine to lysine and alpha-ketoglutarate, the last step in lysine biosynthesis. Defects in LYS1 give rise to a group of

metabolic disorders including saccharophinuria associated with hyperlysinaemia and lysinuria. It is an autosomal recessive disorder which can cause neurological problems including spastic diplegia - neuromuscular condition of hypertonia and spasticity in the muscles of the lower extremities of the human body (legs, hips and pelvis) (Menkes et al., 2006).

1.4 Peroxisomal proteins selected for study

The work in this thesis is focused on three peroxisomal proteins including the enzymes GPD1 and LYS1 and the peroxin PEX7.

1.4.1 Glycerol-3-phosphate dehydrogenase1 (GPD1)

Cells as well as entire organisms are equipped with mechanisms to adapt to sudden and severe changes of the environment which are usually termed as stress conditions. In general, the adaptation to sudden changes of water availability in the environment is essential for survival in nature, and is referred to as the osmostress response (Mager and Varela, 1993).

One form of this response which takes place in yeast is the accumulation of glycerol (Blomberg and Adler, 1992) produced by enhanced levels of GPD1, making the enzyme crucial for growth under osmotic stress (Larsson et al., 1998). Moreover, the study of genome-wide monitoring of transcript changes in yeast under various conditions have shown that GPD1 belongs to a large group of common stress-response genes, and accordingly, its expression is altered by a wide variety of stresses, including heat, cold and oxidative stress (Boy-Marcotte et al., 1999; Panadero et al., 2006; Godon et al., 1998). The apparent complexity of GPD1 regulation and its control by multiple signalling

pathways (Rep et al., 1999) speaks to the complexity of stress responses in yeast (Koerkamp et al., 2002; Brauer et al., 2005).

GPD1 is a NAD^+ -dependent glycerol 3-phosphate dehydrogenase1 which is usually considered to be a cytosolic protein, although, quantitative mass spectrometry of the *S. cerevisiae* peroxisomal proteome and live cell fluorescence microscopy identified a pool of GPD1 in peroxisomes (Marelli et al., 2004; Valadi et al., 2004). In addition, examination of the amino acid sequence of GPD1 shows that its N-terminus contains a sequence of amino acids that conforms to the consensus sequence for the PTS2 (Platta and Erdmann, 2007), and the importance of this sequence in binding to PEX7 was confirmed (Aitchison et al., 2010).

Significantly, localization of GPD1 to peroxisomes is dependent on the metabolic status of cells and the phosphorylation of aminoacyl residues adjacent to the targeting signal. This was revealed in a global proteomic analysis in yeast that identified a phosphorylated peptide derived from GPD1 in which Ser24 and Ser27, adjacent to the PTS2 sequence, were phosphorylated (Aitchison et al., 2010). Moreover, GPD1 dynamically changes its subcellular distribution among the cytosol, peroxisome and nucleus depending on the type of cellular stress. It is primarily cytosolic, but exposure to the fatty acid, oleic acid, changes its localization to the peroxisome, while exposure of cells to osmotic stress changes it to the nucleus (Aitchison et al., 2010).

GPD1 is one of the two NAD^+-dependent glycerol 3-phosphate dehydrogenases in yeast (Larsson et al., 1993) that catalyzes the conversion of dihydroxyacetone phosphate (DHAP) to glycerol 3-phosphate (Larsson et al., 1998) (Figure 1-6). In unstressed cells, this reaction prevents the accumulation of DHAP which can otherwise be transformed

into methyl glyoxylate, a toxic compound that can react with proteins affecting their function (Martins et al., 2001). This reaction also allows for the reoxidation of NADH to NAD^+ which can serve as a buffer for cytosolic redox balance, compensating for cellular reactions that produce NADH (Larsson et al., 1998). Furthermore, glycerol-3-phosphate is a key metabolite for the synthesis of glyceride lipids and phospholipids, as well as for the formation of glycerol (Beopoulos et al., 2008).

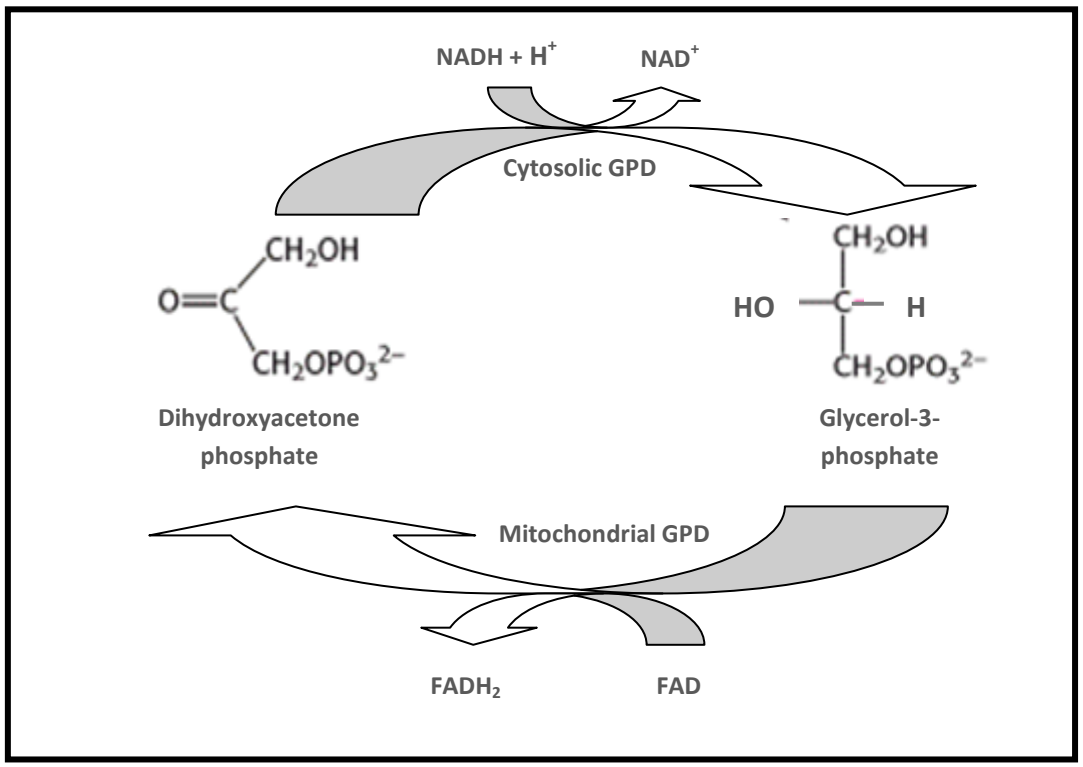

Figure 1-6: Catalytic conversion of dihydroxyacetone phosphate to glycerol-3-phosphate.

To identify structures with possible similarity to *Saccharomyces cerevisiae* protein GPD1 (YDL022W), the GPD1 sequence was compared against protein sequences in the RCSB Protein Databank (PDB) using the Smith-Waterman program (Smith and Waterman, 1981). There were 15 PDB homologs found for GPD1 of which human GPD1

showed the highest sequence similarity (50% identical, 26% similar). The crystallographic asymmetric unit of human GPD1 contains two monomers that form a dimer with a non-crystallographic 2-fold axis. Furthermore, this was supported by Superdex 200 gel filtration experiments which clearly indicated the presence of a dimer in solution. The monomer is organized into two distinct domains, an eight-stranded β-sheet sandwich domain and a C-terminal helical domain (Figure 1-7) [as observed in many other structures of NAD (P)-dependent dehydrogenases] (Zihe et al., 2006).

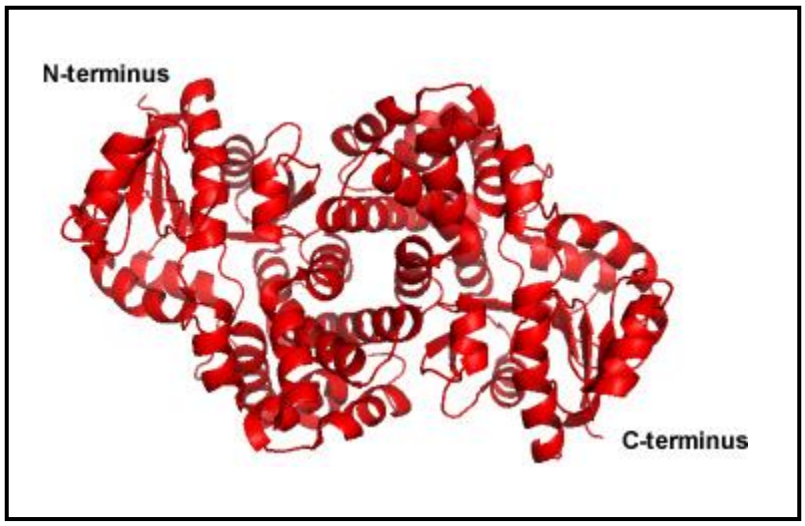

Figure 1-7: Cartoon representation of the structure of human GPD1; Structure of human GPD1 (PDB accession number 1XOV) oriented along the non-crystallographic two-fold axis of symmetry.

1.4.2 Saccharopine dehydrogenase1 (LYS1)

Lysine is an essential amino acid which is synthesized by humans, many plants, bacteria and fungi. Two different biosynthetic pathways have evolved in nature to produce lysine (Bhattacharjee, 1985). (1) The diaminopimelate pathway is found in a wide range of plants, bacteria and lower fungi. This pathway has been a target for the development of antibacterials because of its importance in the synthesis of bacterial cell wall components (Berges et al., 1986).

(2) LYS1, one of the foci of this thesis, is part of the second lysine biosynthetic pathway, also called the α-aminoadipate pathway, which is unique to the euglenoids and higher fungi (Zabriskie and Jackson, 2000). Although the enzymes of this pathway are unique to lysine synthesis, they have some similarities to parts of the pathway of bacterial arginine synthesis (Bhattacharjee, 1992) leading to a focus on the pathway as a possible means of controlling the growth of fungal pathogens (Palmer et al., 2004).

Of seven enzymes, the terminal enzyme of the α-aminoadipate pathway, saccharopine dehydrogenase (LYS1) (Xu et al., 2006), is probably the most extensively studied enzyme. It catalyzes the reversible NAD-dependent oxidative cleavage of saccharopine to yield L-lysine and α-ketoglutarate (α-KG) (Figure 1-8).

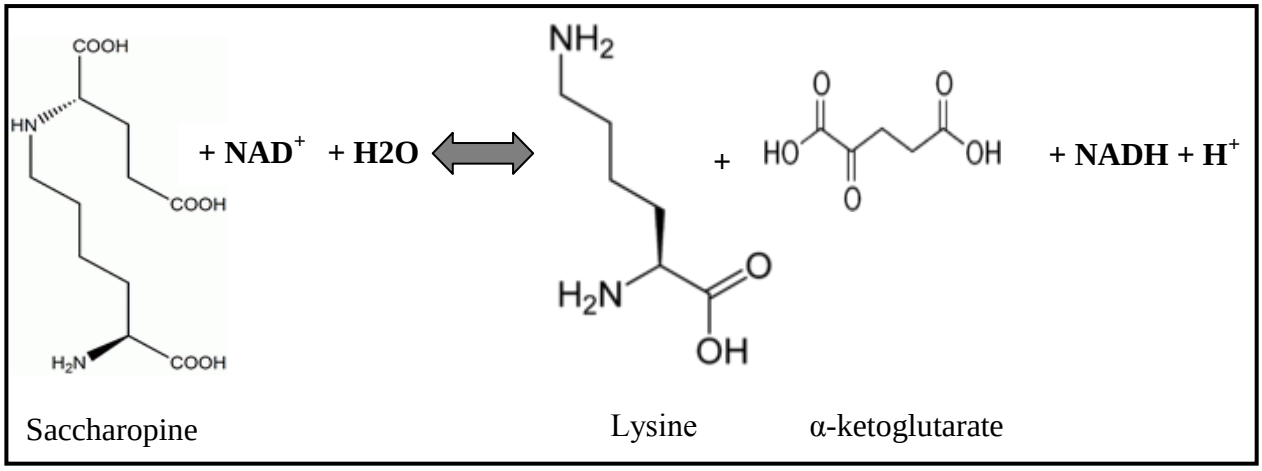

Figure 1-8: Catalytic conversion of saccharopine to lysine and α-ketoglutarate.

LYS1 is among the genes that are upregulated by a factor of 2.56 in response to a disruption of PEX12, a key component of peroxisomal protein import, the absence of which prevents peroxisome formation (Krisans et al., 2002; Albertini et al., 2001). Moreover, LYS1 contains a C-terminal PTS1 signal sequence and is targeted to the peroxisome in a PEX3 dependent manner (Geraghty et al., 1999). Surprisingly, other enzymes in the lysine biosynthetic pathway are not targeted to the peroxisome (Krisans et al., 2002)) raising questions about the role of LYS1 in the peroxisome.

The crystal structure of yeast LYS1 was reported shortly after work on this project was initiated (Berghuis et al., 2007). It is folded into two domains, I (residues 2-134 and 326-373) and II (residues 135-325) with a narrow cleft between them (Figure 1-9). The two domains are similar in structure containing both beta-sheet and helical regions.

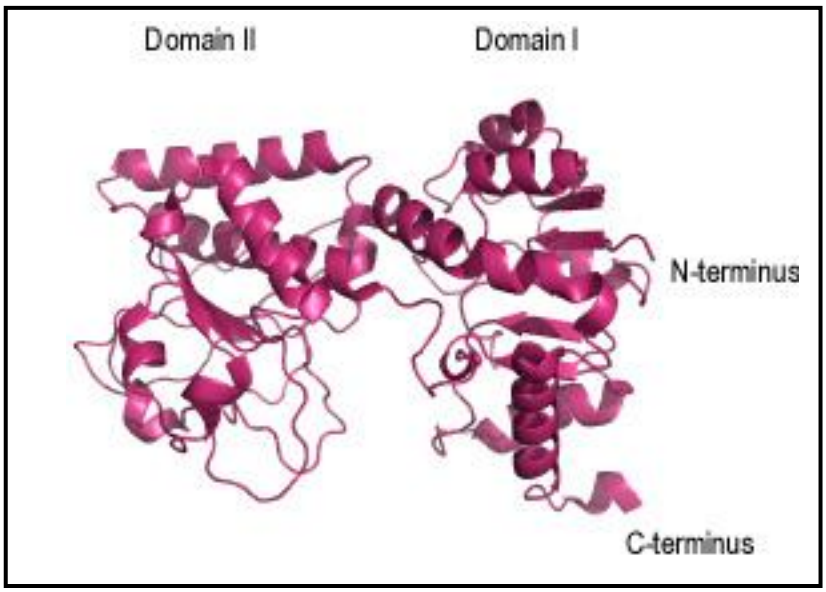

Figure 1-9: Cartoon representation of the structure of saccharopine dehydrogenase from *S. cerevisiae;* Structure of yeast LYS1 (PDB accession number 2Q99) oriented to illustrate the two domains.

1.4.3 Peroxin7 (PEX7)

PEX7, initially discovered in *Saccharomyces cerevisiae* (Marzioch et al., 1994), is characterized by the presence of six WD40 motifs (Zhang et al., 1995). Studies have shown that phenotypically, PEX7 mutants have morphologically normal peroxisomes and normal import of PTS1 proteins but impaired import of PTS2 proteins, such as 3-ketoacyl-CoA thiolase. As described above, PEX7 interacts directly with the PTS2 signal sequences and is the receptor protein for PTS2 proteins (Rehling et al., 1996).

In addition to its key role as a receptor protein, PEX7 is interesting for other reasons. The first is that a deficiency in PEX7 is manifested in Rhizomelic chondrodysplasia punctata (Braverman *et al.*, 1997; Motley *et al.*, 1997; Purdue *et al.*, 1997) and can also cause Refsum disease (van den Brink *et al.*, 2003). This classifies these severe disorders of peroxisomal biogenesis as diseases of protein targeting and emphasizes the critical role of PTS2 targeting in peroxisomal biogenesis. The second is that PEX7 differs from PEX5, in that it appears to act as a simple shuttle, transporting proteins to the membrane where interactions with PEX18 and PEX21, followed by PEX13 and PEX14 complete the process (Stein et al., 2002). The role of PEX7 in mammals where PEX18 and PEX21 do not exist (Dodt et al., 1995) may differ from that in yeast involving an extended shuttle mechanism (Dammai and Subramani, 2001) wherein a mobile receptor enters the peroxisomal matrix during the course of its normal functions and reemerges to the cytosol for another round of transport.

Attempts to identify PEX7's intracellular location, whether in the cytosol or the peroxisome, have been inconclusive, apparently caused by the choice of label. In yeast and human fibroblasts, N-terminally Myc-tagged PEX7 was found predominantly in the

cytosol (Marzioch et al., 1994; Braverman et al., 1997), whereas, PEX7, C-terminally tagged with three copies of HA epitope, was localized entirely inside the peroxisomes in *S. cerevisiae* (Zhang and Lazarow, 1995). Indeed, Pex7 with a C-terminal GFP tag was localized to the peroxisomes in the mammalian cells with substantial cell to cell variation in the amount of PEX7-GFP in the cytosol (Ghys et al., 2002). Accordingly, it has been proposed that PEX7 may function as an intraperoxisomal pulling receptor or as a cytosol-to-peroxisome shuttling receptor, leaving the PEX7 mechanism open to conjecture.

1.5 Objective of thesis

The long term goal of the research is to characterize structurally the peroxisomal proteins. The objective of the work in this thesis was to express, purify and take to crystallization trials GPD1, LYS1 and PEX7.

2. MATERIALS AND METHODS

2.1. Biochemical and common reagents

All chemicals, reagents and antibiotics used in the course of this study were of the highest grade available and unless otherwise stated, purchased from either Fisher Scientific Ltd. (Mississauga, Ontario) or Sigma Chemical Co. (St. Louis, Missouri). PCR reaction kits, restriction enzymes and buffers and T4 DNA ligase were purchased from Invitrogen Canada Inc. (Burlington, Ontario). Media components used for growth of *E. coli* cultures were purchased from DIFCO (New Jersey, USA). Growth media were prepared using reverse osmosis distilled water and all other solutions were prepared with MilliQ water (Millipore Co., Billerica, Massachusetts).

2.2. *Escherichia coli* strains and plasmids

The *Saccharomyces cerevisiae GPD1*, *LYS1* and *PEX7* genes were inserted into plasmid pKS- to generate the pKS-GPD1, pKS-LYS1 and pKS-PEX7 plasmids. *E. coli* Strains, NM522 and JM109 were routinely used for cloning and plasmid propagation. For double-stranded DNA sequencing, usually plasmid DNA isolated from JM109 was used. The genes were then transferred into plasmid pET28b+ to generate plasmids to be used for protein expression. The *E. coli* strain BL21 (λDE3) was used for expression of the recombinant GPD1, LYS1 and PEX7 proteins. *E. coli* BL21 (λDE3) has genome-encoded T7 RNA polymerase which is under the control of lacUV5 promoter. IPTG acts as a substrate analogue of allolactose and it was used to activate the lacUV5 promoter to produce mRNA encoding the recombinant proteins. The Rosetta (DE3) strain was also used for expression of the recombinant PEX7 protein. This strain is a BL21 derivative designed to enhance the expression of eukaryotic genes that contain codons (AUA, AGG,

AGA, CUA, CCC, GGA), rarely used in *E. coli*. The *E. coli* strains and plasmids used in this study are listed in Table 2.1.

Table 2-1: Genotypes and sources of *Escherichia coli* strains and plasmids used in this study.

	Genotype	**Source**
***E. coli* strains**		
NM522	*sup*E Δ(*lac-pro*AB) *hsd*-5 [F' *pro*AB *lac*I^q *lac*Z Δ 15]	Mead et al. (1985)
JM109	recA1 *sup*E44 *end*A1 *hsd*A1 *had*R17 *gyr*A96 *rel*A1 *thi* Δ(lac-*pro*AB)	Yanisch-Perron et al. (1985)
BL21	F^- *omp*T *gal dcm lon hsd*S_B ($r_B^- m_B^-$) λ(DE3) pLysS (cm^R)	Davanloo et al. (1984)
Rosetta (DE3)	F^- *ompT hsdS*$_B$ ($r_B^- m_B^-$) *gal dcm* (DE3) $pRARE^2$ (Cam^R)	Novagen (2001)
Plasmids		
pKS-*	Amp^R	Stratagene Cloning System
pET28b+	Kan^R	Novagen Cloning System

* pBluescript™

2.3. Culture media and storage media

E. coli cultures were grown in Luria-Bertani (LB) media containing 10 g/L tryptone, 5 g/L yeast extract and 5 g/L NaCl. Solid LB media contained 10 g/L agar. Long term storage of cultures was accomplished by adding 24% dimethylsulfoxide or 30% glycerol before freezing at -60 ^{o}C.

2.4. Antibiotic concentrations in the growth media

Ampicillin was added to a concentration of 100 µg/mL for selection of plasmid containing cells. For the plasmid carrying the kanamycin resistance gene, kanamycin was added to a concentration of 40 µg/mL. For the strain Rosetta (DE3), 40 µg/mL of chloramphenicol was added for selection of plasmid containing cells.

2.5. DNA manipulation

2.5.1. DNA isolation and purification

Plasmid DNA was isolated according to Sambrook et al., (1989) and all procedures were carried out at room temperature. The plasmids harbouring the gene of interest (i.e. GPD1, LYS1 and PEX7) were obtained cloned into the plasmid pBG1805 (Grayhack et al., 1999) transformed into *E. coli* DH5α. The strains were inoculated and grown overnight in 5 mL LB cultures in the presence of an appropriate concentration of ampicillin. Approximately 3 mL of the cultures were pelleted by centrifugation using a bench top centrifuge (IEC Micro MB) and resuspended in 200 µL of glucose-EDTA-RNase buffer (25 mM Tris-HCl pH 8.0, 1% glucose, 10 mM Na-EDTA and 0.35 mg/mL RNase). The cells were then lysed with 400 µL of a solution of 1% SDS and 0.2 M NaOH. After a 10 minute incubation, 300 µL of 6.3 M ammonium acetate was added and the mixture was centrifuged twice to remove all precipitate. Plasmid DNA was then

precipitated by the addition of 550 µL isopropanol. After a 15 minute incubation, plasmid DNA was pelleted by centrifugation, washed twice with 70% ethanol, and dried under vacuum. The DNA pellet was resuspended in either water or TE buffer (10 mM Tris pH 8.0, 1 mM Na-EDTA) and stored at -20 ^{o}C until needed.

2.5.2. PCR amplification

The primers outlined in Table 2.2 were (Invitrogen Inc. Canada) dissolved initially in 20 µL of DNase-RNase free water and then diluted to 40 pM before storage at -20 ^{o}C. A DNA Thermal cycler (Perkin Elmer Cetus Company) was used for

Table 2-2: Oligonucleotide primers used for PCR amplification.

ORF	Primer	Oligonucleotide sequence
YDL022W	GPD1-F	AGCAGAATTCCATATGTCTGCTGCTGC
	GPD1-R	AAGAAGGATCCTTAATCTTCATGTAG
YDR142C	PEX7-F	GCAGGGAGCTCAATGCTCAGATATCA
	PEX7-R	AAGAACTCGAGTTAACCTAAGCCGTT
YIR034C	LYS1-F	AGCAGAATTCCATATGGCTGCCGTCAC
	LYS1-R	AAGAAGGATCCTTACAATCTTGAAGA

Note: Sequence in red is from the ORF and sequence in blue is end of the ORF.

all amplifications including 1X PCR buffer (20 mM Tris-HCl pH 8.4, 50 mM KCl), 0.2 mM dNTPs, 1.5 mM MgCl2, 0.5 µM of both forward and reverse primers, 1 µg of plasmid DNA, and 2.5 units of *Pfu* DNA polymerase (prepared by Jack Switala). Autoclaved water was used to make up for the volume to 100 µL. 50 µL of light mineral

oil was added to the top of the reaction mixture to prevent evaporation. The reactions normally involved 35 cycles of denaturation at 98 ^{o}C for 45 seconds, primer annealing at 50 - 55 ^{o}C for 30 seconds and primer extension at 68 to 72 ^{o}C for 90 seconds. The final elongation was at 72 ^{o}C for 5 minutes after which the mixture was kept at 4 ^{o}C until separation.

2.5.3. Agarose gel electrophoresis

Electrophoresis of the amplified reaction mixture was performed according to Sambrook et al., (1989). Agarose gels containing 1% Agarose and 0.1 µg/mL ethidium bromide were prepared in TAE buffer (40 mM Tris-acetate and 1 mM EDTA, pH 8.0) and cast in Bio-Rad Mini Sub Cell Plexiglass horizontal electrophoresis trays (6.5cm × 10cm). Samples of 10 µL volumes were mixed with 2 µL stop buffer (40% glycerol, 10 mM EDTA pH8.0, 0.25% bromophenol blue). 1Kb Plus^{TM} DNA Ladder (Invitrogen Inc. Canada) served as molecular weight size standards. Electrophoresis was carried out at 45-50 mA constant current in TAE buffer until the bromophenol blue dye marker front had migrated approximately two-thirds the length of the gel. The DNA bands were visualized with ultraviolet light and recorded using a Gel Doc 1000 image capture (Bio-Rad, Minneapolis, USA).

2.5.4. Restriction endonuclease digestion of DNA

The DNA fragments to be digested were excised from agarose gels and purified using the Ultraclean^{TM} 15 DNA purification kit (gene clean kit) from Bio/Can Scientific Inc. (Mississauga, Ontario) according to the instructions supplied by the manufacturer. The purified insert and pKS- vector DNA samples were subjected to restriction digestion. Restriction digestions were performed at 37 ^{o}C for 2-5 hours in a total volume of 10 µL,

containing 1 µL of 10X of the appropriate buffer provided by the supplier, 1-5 µg DNA and 0.5-1 µL of the appropriate endonuclease(s).

2.5.5. Ligation

Agarose gel electrophoresis was carried out for the digested samples of insert and vector. The DNA fragments to be ligated were excised from agarose gels and purified using the gene clean kit. Ligation of DNA fragments was carried out according to the procedure of Sambrook et al. (1989). Purified DNA fragments were mixed in a ratio of 1-3 of insert to vector in 10 µL volumes, containing 1 µL of T4 DNA ligase and 2 µL of the manufacturer's supplied ligase buffer (250 mM Tris-HCl pH 7.6, 50 mM $MgCl_2$, 5 mM ATP, 5 mM DTT, 25% (w/v) polyethylene glycol-8000). The ligation mixtures were incubated overnight at 15 ^{o}C before being transformed into NM522. A mixture without the insert DNA was used as a negative control.

2.5.6. Transformation

Transformation of *E. coli* cells with plasmid DNA was done according to Chung et al. (1989). The NM522 strain of *E. coli* cells was grown to exponential phase (typically 2-4 hours) in 5 mL LB cultures, harvested by centrifugation and rendered competent by resuspension in 500 µL of ice-cold 0.1 M $CaCl_2$. After a minimum incubation on ice of 30 minutes, 2-10 µg of plasmid DNA was added to 100 µL of the cell suspension, followed by a further 30 minute incubation on ice, and a 90 second heat shock at 42 ^{o}C. Ice-cold LB medium (900 µL) was then added to the cell suspension and incubated at 37 ^{o}C for 1 hour. The mixture was either spread, or in the case of ligation mixtures, mixed with 3 mL of molten R-top LB agar and poured onto an appropriate antibiotic containing LB plate which was incubated at 37 ^{o}C for 16 hours.

Four to eight colonies were usually screened and a plasmid with the correct restriction pattern was subsequently transformed into JM109. Since, JM109 is *rec*A- and the endonucleaseA mutation leads to an improved yield and quality of isolated plasmid DNA, it gives better sequencing results compared to NM522. After screening, a plasmid with the known restriction pattern was subjected to DNA sequencing to confirm that no mistakes had been introduced during PCR replication.

2.5.7. DNA sequencing

Automated sequencing was carried out on an Applied Biosystems model 3130 Genetic Analyzer. The DNA to be sequenced was isolated and purified as described above except the DNA pellet was resuspended in water instead of TE buffer as recommended by the instructions in the BigDye® Terminator v1.1 Cycle Sequencing Kit (Applied Biosystems). The sequencing reaction mixture contained approximately 200 ng of DNA with 3 pmol of the appropriate primer and sequencing was carried out as directed in a final volume of 20 µL. The PCR cycle program for the sequencing reaction included a preheat step for 1 minute followed by 25 cycles of denaturing, annealing and extension steps respectively at 96 ^{o}C for 10 seconds, 50 ^{o}C for 5 seconds and 64 ^{o}C for 4 minutes, followed by cooling to 4 ^{o}C. The DNA was then purified by precipitation by the addition of 2 µL of 125 mM EDTA, 2 µL of 3 M sodium acetate pH4.8, 60 µL of 95% ethanol and gently mixed by inversion. After 15 minute incubation at room temperature, the DNA was recovered by centrifugation at 4 ^{o}C for 15 minutes. The supernatant was carefully recovered by pipetting and 60 µL of 70% ice cold ethanol was added and centrifuged at 4 ^{o}C for 15 minutes. The supernatant was again removed by pipetting and the final pellet was dried for a minimum of 30 minutes under vacuum. Finally, the purified DNA pellet

was denatured by addition of 20 µL of Hi-Dye formamide, thoroughly mixed by vortexing and incubated at 94 ^{o}C for 5 minutes before being loaded into the sample plate for automated sequencing on a 3130 Genetic Analyzer (Applied Biosystems, Canada). Finally, the sequence was verified manually.

2.5.8. Cloning in pET28b+ vector

After the sequence was verified to be correct, the insert was removed from the pKS- vector with specific restriction enzymes and ligated into pET28b vector which was digested with the same enzymes (Table 2.3) as described above. Eventually, transformation of *E. coli* BL21 cells with the plasmid DNA was done as described above. A plasmid with the correct restriction pattern was identified and an aliquot of the respective culture was stored in 24% DMSO at -60 ^{o}C. The PEX7-contianing plasmid was also transformed into Rosetta (DE3) cells.

Table 2-3: Protein expression plasmids used over the course of the study.

Plasmid	Cloning restriction sites	Purification tag
pET28b-GPD1	*Bam*HI/*Nde*I	6X His-tag
pET28b-LYS1	*Bam*HI/*Nde*I	6X His-tag
pET28b-PEX7	*Sst*I/*Xho*I	6X His-tag (N- and C-terminal)

2.6. Recombinant protein expression

Before large scale purification, plasmid-containing BL21 or Rosetta (DE3) cells were grown in small 30 mL flasks of LB medium at 37 ^{o}C until the OD at A_{600} was

approximately 0.6. This was followed by induction with IPTG at either high (1 mM) or low (0.1 mM) concentration to induce RNA and protein synthesis; the induced cultures were grown at room temperature, 28 ^{o}C and 37 ^{o}C, as part of the screening process to identify the optimum conditions. Whole cells as well as crude extracts were tested for protein expression by electrophoresis on sodium dodecyl sulphate polyacrylamide gels (SDS-PAGE). The inductions of GPD1 and LYS1 and their expressions in crude extracts were best with 0.1 mM IPTG. The expression of PEX7 was found to be more promising in Rosetta (DE3) cells compared to BL21 cells and 1 mM IPTG at 28 ^{o}C produced the most efficient induction.

2.7. Recombinant protein purification

For large scale purifications, cells transformed with the plasmids expressing the desired proteins were grown at 28 ^{o}C in 500 mL culture volumes of LB medium in 2 L shake flasks supplemented with 40 µg/mL of kanamycin and induced with suitable concentrations of IPTG, based on the small scale expression, for around 16 hours with good aeration. Cells were harvested from the growth medium by centrifugation at 7000 rpm for 10 minutes and the cell pellets were stored at -60 ^{o}C if purification was not started immediately.

The cell pellet was resuspended in 50 mM potassium phosphate buffer, pH7 (for GPD1 and PEX7) or 50 mM Tris buffer, pH8 (LYS1), both containing 5 mM EDTA in a ratio of 75 g cells to 400 mL buffer. The cells were disrupted by a single or double pass through a French pressure cell at 20,000 psi. Unbroken cells and debris were removed by centrifugation, yielding the crude extract, to which streptomycin sulphate was added to a final concentration of 2.5%. The resulting precipitates were removed by centrifugation

and discarded. Solid ammonium sulphate was added starting at a concentration of 30%, incrementally increasing by 10% up to 70%, removing the precipitate by centrifugation at each step. The protein pellets from ammonium sulphate precipitations were resuspended and the presence of the desired proteins in the pellets was confirmed by SDS-PAGE gels. Resuspensions were centrifuged to remove any remaining precipitates, and dialyzed overnight using a 12,000 – 14,000 molecular weight cut-off membrane, against 2 litres of suitable buffers.

Rosetta (DE3) cells transformed with the plasmids expressing PEX7 protein were grown at 28 ^{o}C in 4 liters of LB media supplemented with 40 µg/mL of kanamycin and induced with 1 mM of IPTG for around 16 hours with good aeration. Cells were harvested from the growth medium by centrifugation at 7000 rpm for 10 minutes and the cell pellets were stored at -60 ^{o}C for further purification steps.

2.7.1. Purification of GPD1

GPD1 was found to precipitate at 50% ammonium sulphate saturation.

Ion Exchange Chromatography (IEC): This is based on a reversible interaction between a charged molecule in solution and an oppositely charged group on the matrix. Initially, it was used to separate basic proteins (Hirs et al., 1951), but later with the introduction of cellulose-based matrices, e.g., carboxymethyl (CM) and diethylamino-ethyl (DEAE), this technique was extended to separate a wide range of proteins (Sober and Peterson, 1956). DEAE is a positively charged resin (weak anion exchanger; pH 3-8) and is used in protein and nucleic acid purification. The gel matrix beads are derivatized with DEAE and therefore, lock negatively charged proteins into the matrix until released by an increasing gradient of salt concentration.

After overnight dialysis, the resuspension was centrifuged again and loaded onto a 2.5 cm × 25 cm column of DEAE-cellulose A-500 (Chisso, America) equilibrated with 50 mM potassium phosphate, pH 7.0. Only fractions containing GPD1 (with highest purity) were pooled and concentrated under nitrogen in a stirred pressure cell (model 8050, Amicon) using a YM-30 membrane to a protein concentration of about 35-40 mg/mL. The concentrated sample was dialyzed against 1 litre of 50 mM potassium phosphate, pH 7.0 overnight. The final dialyzed protein was checked for purity by SDS-PAGE. Purified protein samples were aliquoted into microcentrifuge tubes in 250 µL volumes and stored at -60 ^{o}C until needed.

2.7.2. Purification of LYS1

LYS1 was found to precipitate at 50% and 60% ammonium sulphate saturation. After overnight dialysis, the resuspension was centrifuged again to clarify. Initial attempts to purify LYS1 involved ion exchange chromatography on DEAE cellulose (as described above) followed by affinity chromatography on 1 mL HiTrap nickel columns (GE Health Sciences Inc., Canada).

Immobilized Metal-ion Affinity Chromatography (IMAC): This is a useful protein purification technique which is based on the interaction of histidine, cysteine, and tryptophan side-chains with the transition metal ions, e.g., Cu^{2+}, Ni^{2+}, Co^{2+}, Zn^{2+} immobilized via iminodiacetic acid to a porous chromatographic support (Belew and Porath, 1990). HiTrap chelating columns are packed with highly cross-linked agarose-beads to which iminodiacetic acid (IDA) has been coupled by stable ether groups via a spacer arm (seven-atoms). Although, imidazole and histidine share the same functional group (imidazol ring), nickel has higher affinity for imidazole than histidine. Therefore,

elution of the desired protein (His-tag) is achieved by increasing the imidazole concentration.

The HiTrap nickel column (1 mL) was first washed with 5ml of distilled water. It was charged with 0.1 M nickel sulfate solution followed by washing once again with 5 mL distilled water. Then, the resin was equilibrated with binding buffer of 50 mM Tris pH 8.0 containing 0.5 M NaCl which was followed by loading the protein sample from ammonium sulphate saturations. The desired protein was eluted with the step-up gradient of imidazole in binding buffer and fractions were checked by SDS-PAGE.

Subsequently, a nickel-nitrilotriacetic acid (Ni-NTA) Superflow resin (Qiagen) in a XK-16 column (Amersham Biosciences Inc., Canada), was investigated. NTA has four chelation sites for nickel ions and therefore, it binds more tightly than IDA which has only three sites available for interaction with nickel. The extra chelation site prevents nickel-ion leaching and results in greater binding capacity, hence, higher protein purity. After clarification, around 150 mg of protein was loaded on the resin (~50 mg/mL capacity) which was then washed with 8-10 column volumes of binding buffer followed by elution with the step-up gradient of imidazole in binding buffer. After confirming the presence of pure LYS1 in the fractions by SDS-PAGE, selected fractions were pooled and concentrated under nitrogen in a stirred pressure cell (model 8050, Amicon) using an YM-30 membrane, to a protein concentration of about 6-8 mg/mL. The concentrated protein was dialyzed against three changes of 1litre of 50 mM Tris, pH 8.0 in a period of 10-12 hours to remove imidazole. The final dialyzed protein solution was clarified by centrifugation and checked for purity by SDS-PAGE. Purified protein samples were aliquoted into microcentrifuge tubes in 500 µL volumes and stored at -60 ^{o}C until needed.

2.7.3. Purification of PEX7

Several protocols were investigated for the purification of PEX7 from the crude extract of plasmid-containing BL21 cells. PEX7 was found to precipitate at 50%, 60% and 70% ammonium sulphate saturation. Fractions were dialysed and centrifuged to clarify. Initial attempts to purify this protein involved both size exclusion chromatography and affinity chromatography involving nickel column (as described above). Moreover, ion exchange chromatography on DEAE cellulose was also investigated.

Size exclusion chromatography was also attempted using Superose 12. The resin (particle size 11 μm, optimal separation range M_r 1kD–300kD) was equilibrated with 50 mM Tris-HCl pH 8.0, 150 mM NaCl, after which 5 mg of dialyzed protein was loaded and eluted. A constant flow of 0.2 mL/min was applied and 0.2 mL fractions were collected. 5 μL of each sample was analyzed by SDS-PAGE. Samples containing the desired protein were pooled, concentrated and purified on a nickel column.

A denaturing protocol was also investigated for PEX7 purification. Cells were resuspended in 50 mM Tris pH 8.0 and disrupted by a single or double pass through a French pressure cell at 20,000 psi. The cell debris was separated by centrifugation at 12,000 rpm for an hour. It was resuspended in a resuspension buffer containing 500 mM potassium chloride, 10 mM Tris pH 8.0, 10% glycerol and 1 mM dithiothreitol. The cell suspension was sonicated to make it homogeneous. To this, denaturing buffer containing 6 M guanidine hydrochloride, 10 mM Tris pH 8.0, 10% glycerol and 1 mM dithiothreitol, was added. The mixture was vortexed twice to mix while keeping it on ice for 30 minutes. Then, it was centrifuged for an hour at 12,000 rpm and the pellet was discarded.

The protein concentration of the supernatant was determined and after dialysis, approximately 150 mg was loaded on a Ni-NTA column. After a prolonged wash with binding buffer (10 column volumes), protein fractions were eluted subsequently with binding buffer containing 25 mM, 50 mM and 250 mM imidazole and checked on SDS-PAGE. Fractions containing PEX7 were dialyzed overnight at 4 ^{o}C against a renaturing buffer containing 0.5 M potassium chloride, 10 mM sodium citrate pH 6.8, 1 mM dithiothreitol and 10% glycerol.

2.8. *In vitro* binding assay

To analyze the GPD1-PEX7 interaction, GPD1 was loaded on a Ni-NTA column and washed with 5 column volumes of binding buffer (50 mM potassium phosphate buffer, pH 7.0 and 0.5 M NaCl). An equimolar amount of PEX7 from the 50-60% ammonium sulfate fraction was then added to the matrix followed by incubation for an hour. After being washed with 5-10 column volumes of binding buffer, the proteins were eluted sequentially with 25 mM, 50 mM and 250 mM imidazole in binding buffer. The eluted samples were analyzed by SDS-PAGE to confirm the co-elution of GPD1-PEX7 and fractions containing the desired proteins were pooled and concentrated under nitrogen in a stirred pressure cell (model 8050, Amicon) using an YM-30 membrane, to a protein concentration of about 17 mg/mL (1 mL volume). The concentrated protein was dialyzed against three changes of 1 litre of 50 mM potassium phosphate buffer, pH 7.0 in a period of 10-12 hours to remove imidazole. The final dialyzed protein was clarified by centrifugation and checked by SDS-PAGE. Purified protein samples were aliquoted into microcentrifuge tubes and stored at -60 ^{o}C until needed.

2.9. Protein Analysis

2.9.1. Determination of protein concentration

During protein purification, the Warburg-Christian method was used to estimate protein concentration (Warburg and Christian, 1941; Layne, 1957). Purified protein concentrations (mg/mL) were estimated spectrophotometrically (Sambrook et al., 1989) based on the absorbances at 280 nm and 260 nm [protein (mg/mL) = $(1.55 \times A_{280}) - (0.76 \times A_{260})$] using an Ultrospec 3100 (Milton Roy).

2.9.2. Sodium dodecyl sulfate-polyacrylamide gel electrophoresis (SDS-PAGE)

Denaturing SDS-PAGE was carried out according to Weber et al. (1972). Discontinuous 4% stacking and 8-12% separating polyacrylamide gels were cast as vertical slabs of dimensions 10 x 10 cm and 0.5 mm thickness. Samples loaded onto the gels usually contained 5-8 µg of protein. Samples were mixed with equal volumes of reduced sample buffer (3.4 mg/mL NaH_2PO_4, 10.2 mg/mL Na_2HPO_4, 10 mg/mL SDS, 0.13 mM 2-mercaptoethanol, 0.36 g/mL urea and 0.15% bromophenol blue) and boiled for 3 minutes before loading. The protein size marker solution (Benchmark^{TM}, Invitrogen Inc., Canada) was loaded around 7 µL. Gels were run at a constant 150 V until the dye reached the bottom, in a vertical BIO-RAD Mini-Protean II electrophoresis system, using a running buffer containing 14 g/L glycine, 3 g/L Tris base and 1 g/L SDS. Gels were stained with a solution containing 0.5 g/L Coomassie Brilliant Blue R-250, 30% methanol and 10% acetic acid for 1 hour, and then, destained with repeated changes of destaining solution containing 15% methanol and 7% acetic acid until the background was clear. The gels were then soaked in a solution containing 7% acetic acid and 1%

glycerol for 30 minutes before being mounted on 3 mm Whatman paper, covered with clear plastic film and dried at 80 ^{o}C for an hour on a slab gel drier under vacuum.

2.10. Enzyme activity

2.10.1. Enzyme activity of GPD1

The enzymatic activity of GPD1 was determined spectrophotometrically (Ultrospec 3100) by monitoring the reduction in NADH at 340 nm for 5 min in a 1 mL reaction mixture containing 0.1 mM NADH, 0.5 mM dihydroxacetone phosphate, 50 mM Tris-HCl (Harold and Nathan, 1969) and 0.5 to 10 µL of diluted GPD1 at room temperature. One unit of glycerol-3-phosphate dehydrogenase activity is defined as the amount of enzyme that oxidizes 1 µmol of NADH per minute at room temperature.

2.10.2. Enzyme activity of LYS1

The enzyme activity of LYS1 was determined by the method of Ogawa and Fujioka (1978) in a spectrophotometer (Ultrospec 3100) by monitoring the reduction of NADH at 340 nm for 5 minutes in a 1 mL reaction mixture containing 0.1 mM NADH, 0.5 mM L-lysine, 0.2 mM α-ketoglutarate and 0.5 to 5µl of diluted LYS1 at room temperature. One unit of saccharopine dehydrogenase activity is defined as the amount of enzyme that oxidizes 1 µmol of NADH per minute at room temperature.

2.11. GPD1 crystallization and structure determination

Crystals were obtained in 10 to 12 days at 20 ^{o}C by the vapor-diffusion, hanging drop method with 2 µL of a 12-13 mg/mL purified protein solution and 2 µL of the reservoir solution containing 12% polyethylene glycol (PEG-8K), 0.1M Tris-HCl pH 8.5 and 0.3 M magnesium chloride. Diffraction data were obtained from crystals cooled with a nitrogen cryo-stream using a Rigaku RA-Micro7 HFM tabletop rotating anode X-ray

generator and R-AXIS IV^{++} CE detector; Rigaku Corporation. The diffraction data sets were processed using the program MOSFLM and scaled with the program SCALA (Otwinowski and Minor, 1996). A portion of GPD1 structure was solved by molecular replacement using human GPD1 as a probe.

3. RESULTS

The primary objective of this research was to express and purify a selection of proteins from the yeast peroxisome leading ultimately to a solution of their structures by X-ray crystallography in near future. The specific proteins included in this study are glycerol-3-phosphate dehydrogenase 1 (GPD1), saccharopine dehydrogenase (LYS1) and peroxin 7 (PEX7).

3.1. Glycerol-3-phosphate dehydrogenase1

3.1.1. Construction of pET28b-GPD1

The yeast chromosomal clone of GPD1 (Open Biosystems, Huntsville, USA) was used as the starting point for this work. A 1.2 kb DNA fragment resulted from PCR amplification (Fig. 3-1, panel A). Restriction digestion of the cloned plasmid in pKS by *Bam*HI and *Nde*I yielded two bands of pKS (3 kb) and *GPD1* (1.2 kb) on agarose gel (Fig. 3-1, panel B). Moreover, digestion of the cloned plasmid in pET28b by same endonucleases yielded the bands of *GPD1* along with pET28b (5.3 kb) (Fig. 3-1, panel C).

3.1.2. Protein expression

Small cultures of BL21 cells expressing GPD1 were grown at room temperature, 28 ^{o}C and 37 ^{o}C and induced with either 0.1 or 1 mM IPTG. Somewhat surprisingly, there was very little induction using 1 mM IPTG (Figure 3-2, panel A) but very efficient expression with 0.1 mM IPTG (Fig. 3-2, panel B). The 43 kDa band corresponding to GPD1 was strongest at 28 ^{o}C which was chosen as the optimum temperature for induction.

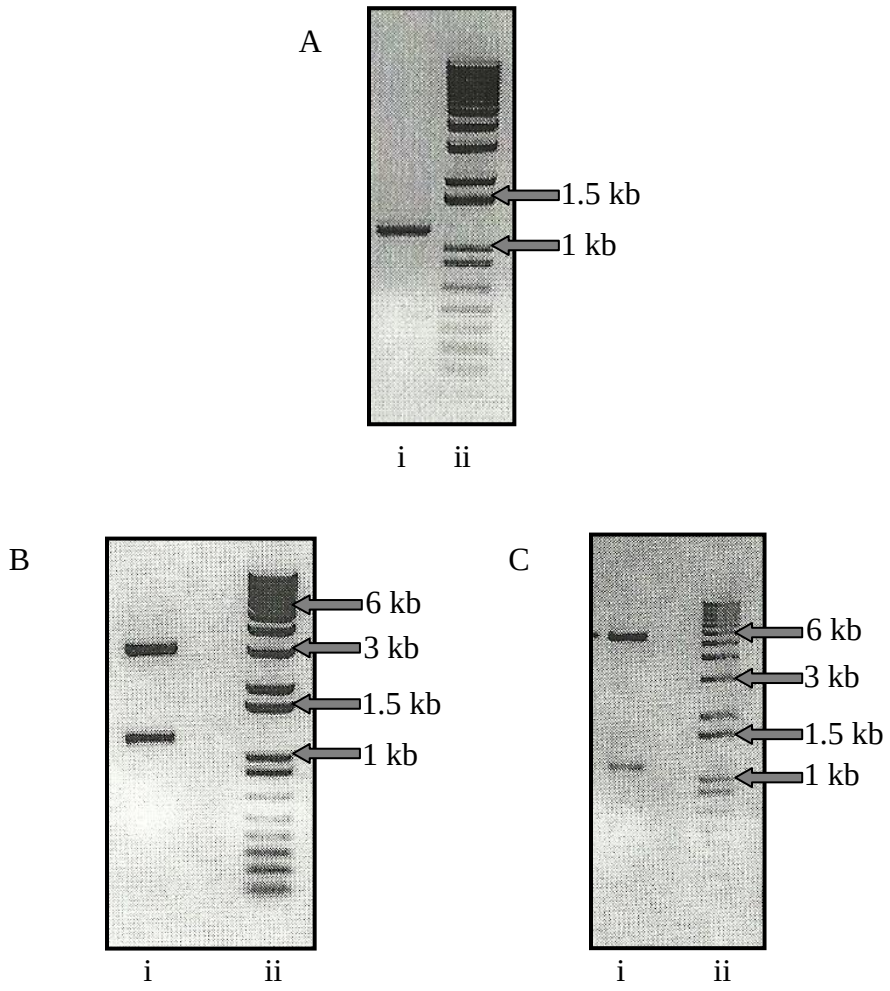

Figure 3-1: Construction of pKS-GPD1 and pET28b-GPD1; (A) Lane i contains the PCR product from the amplification of the GPD1 clone using primers described in the Methods. (B) Lane i contains pKS-GPD1 DNA cut with *Bam*HI and *Nde*I restriction nucleases. The pKS vector migrates at 2.9 kb and the GPD1 insert migrates at 1.2 kb. (C) Lanes i contains pET28b-GPD1 DNA cut with *Bam*HI and *Nde*I restriction nucleases. The pET28b vector migrates at 5.3 kb and the GPD1 insert at 1.2 kb. Lane ii of (A), (B) and (C) contains 1 kb DNA ladder.

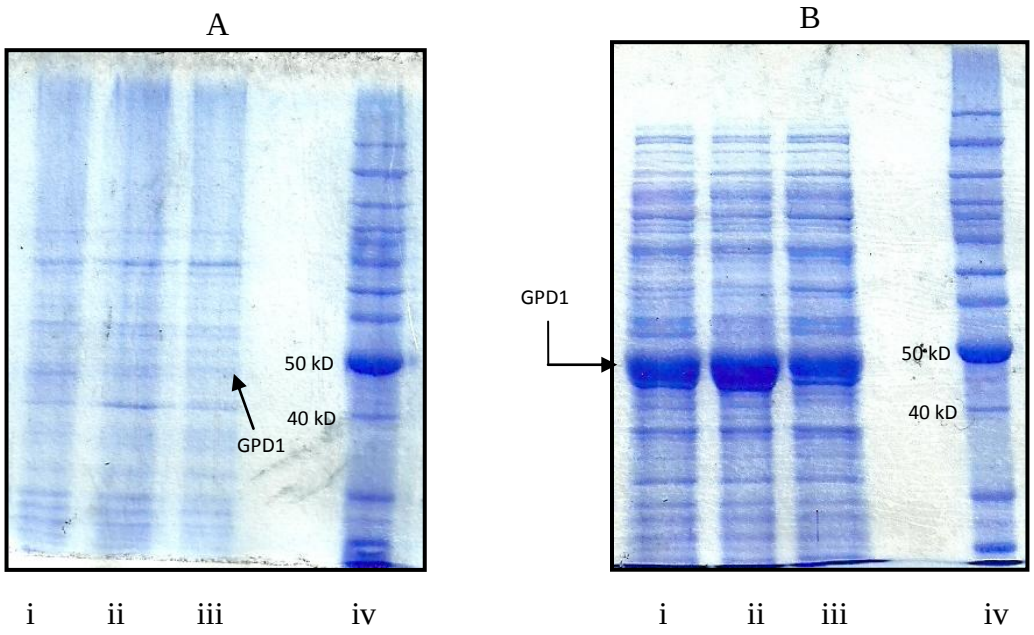

Figure 3-2: Small scale expression trials of GPD1; Lanes i, ii and iii in panels (A) and (B) contain protein from cultures of pET28b-GPD1 transformed BL21 grown at room temperature, 28 ^{o}C and 37 ^{o}C, respectively. The cultures in panel (A) were induced with 1 mM IPTG and the cultures in panel (B) were induced with 0.1 mM IPTG. Lane iv contains the protein size markers in both panels.

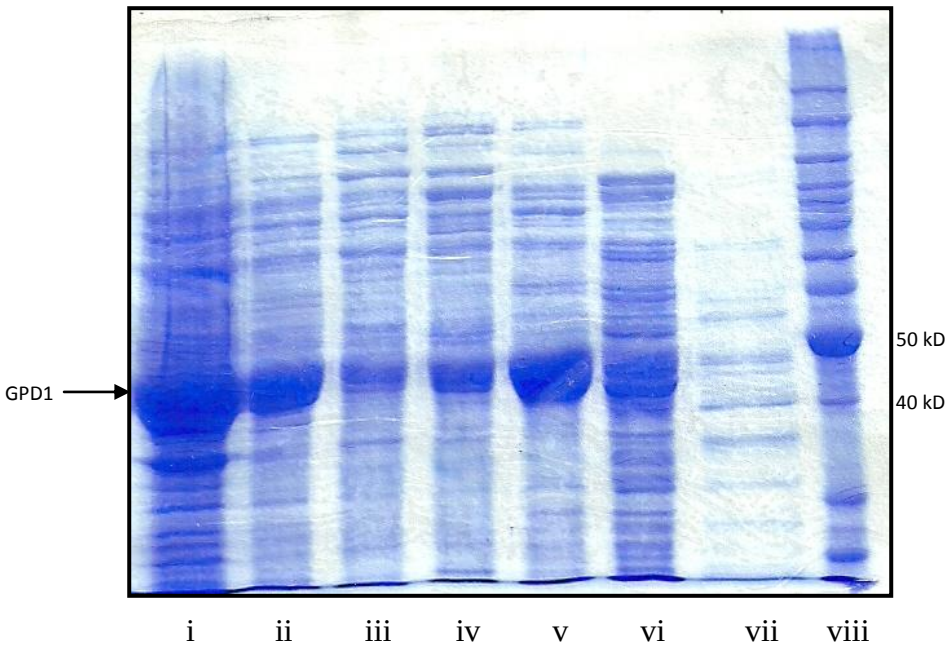

Figure 3-3: Fractionation of GPD1 by ammonium sulfate; Lanes i - vii contain protein fractions from the various stages of GPD1 purification, separated by SDS-PAGE: lane i - crude extract; lane ii - streptomycin sulfate supernatant; lanes iii, iv, v and vi - 30%, 40%, 50% and 60% ammonium sulfate pellets, respectively; lane vii - 60% ammonium sulfate supernatant. Lane viii contains protein size markers.

3.1.3. Protein purification

GPD1 was purified utilizing sequentially, streptomycin sulfate treatment, ammonium sulfate precipitation and ion exchange chromatography on DEAE cellulose. The results of fractionation through ammonium sulfate are shown in Figure 3-3. Following ammonium sulfate precipitation, the 50% saturation of ammonium sulfate fraction was loaded on a Cellufine A500 column as describe in the Methods section. The column was washed with 50 mM potassium phosphate, pH 7 until the absorbance at 280 nm was below 0.025. The protein was then eluted with a linear gradient of 0-500 mM NaCl in 50 mM potassium phosphate pH 7 in a total volume of 1 L. Approximately 5 mL fractions (80 drops) were collected and the protein was assayed at 280 nm revealing two peaks of protein (Fig. 3-4, panel A). SDS-PAGE revealed that the first peak predominantly contained GPD1 (Fig. 3-4, panel B). The purified protein is shown after SDS-PAGE in Fig. 3-4, panel C.

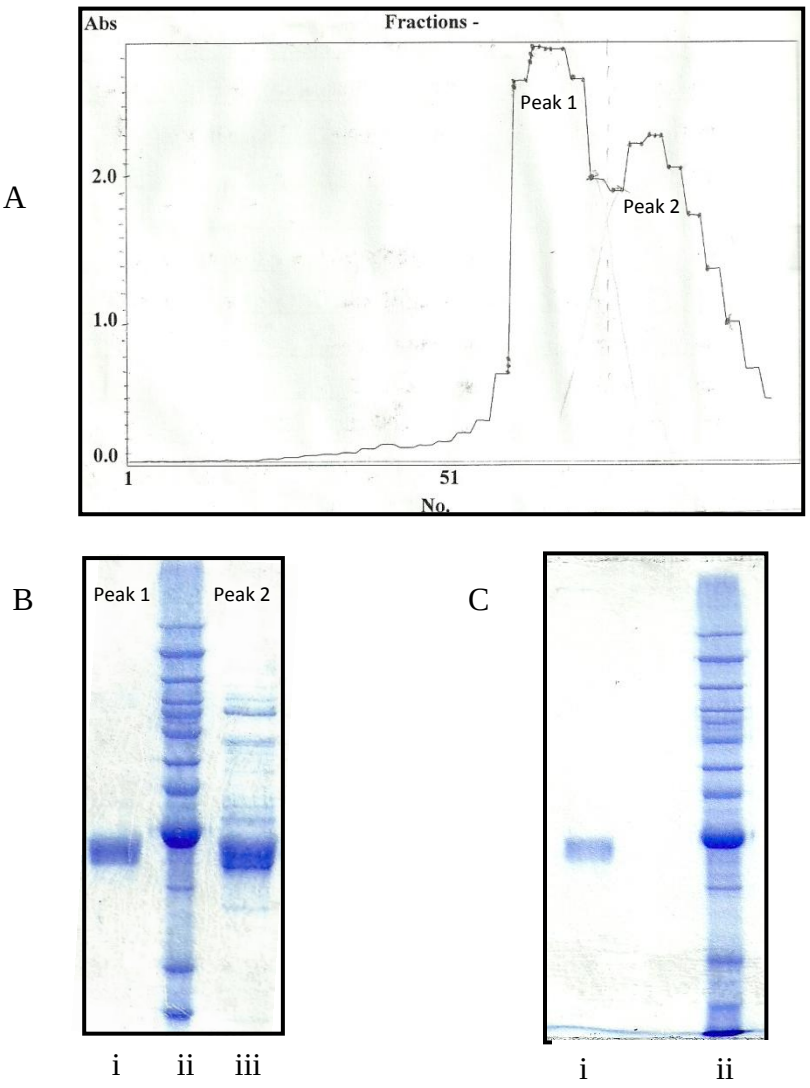

Figure 3-4: Purification of GPD1 on DEAE cellulose; (A) Elution profile of protein assayed at 280 nm. (B) Lanes i and iii contain pooled and concentrated fractions of GPD1 from peak 1 and peak 2 of Fig. A respectively. Lane ii contains protein size markers. (C) Lane i contains 2 micrograms of purified GPD1 fraction and lane ii contains protein size markers.

3.1.4. Enzyme activity of GPD1

The glycerol dehydrogenase activity of GPD1 was determined spectrophotometrically measuring the decrease in NADH absorbance at 340 nm. A specific activity of 0.03 µmol/min/µg was determined which is very similar to the 0.05 µmol/min/µg determined previously (Harold and Nathan, 1969).

3.1.5. Crystallization and structure determination

GPD1 was crystallized by the hanging drop vapour diffusion method with a reservoir solution of 12% polyethylene glycol (PEG-8K), 0.1M Tris-HCl pH 8.5 and 0.3 M magnesium chloride as described in section 2.11. Colorless crystals up to 0.1 mm in size were obtained after 10 - 12 days which were found to belong to the orthorhombic space group C222 (Fig. 3-5). Diffraction data sets were obtained to a resolution of 2.2 Å (Table 3.1) which were used to solve the C-terminal portion of the structure (Fig. 3-6) by molecular replacement using the human enzyme (PDB 1X0V) as probe. The N-terminal 160-180 residues were too disordered or existed in multiple folds preventing a clear definition of that portion of the structure.

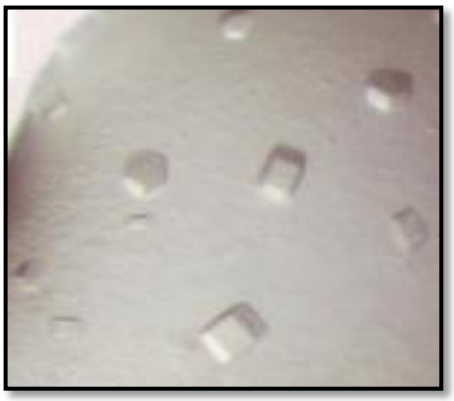

Figure 3-5: Crystals of GPD1 observed by compound microscope and used for data collection.

Table 3-1: Data collection and refinement statistics for GPD1.

Data collection statistics	**Overall**
Unit cell parameters	
a (Å)	84.06
b (Å)	96.25
c (Å)	104.16
α, β, γ (^{o})	90.0
Resolution[a]	40.2 – 2.10
	(2.21 – 2.10)
Unique reflections	22694 (2840)
Completeness (%)	91.0 (79.0)
R_{merge}	0.140 (0.590)
Mean [I/σ_I]	6.1 (2.0)
Multiplicity	4.0 (3.8)
B - Model refinement statistics	
Space group	C222
R_{cryst} (%)	44.4
R_{free} (%)	47.1

[a]Values in parentheses correspond to the highest resolution shell

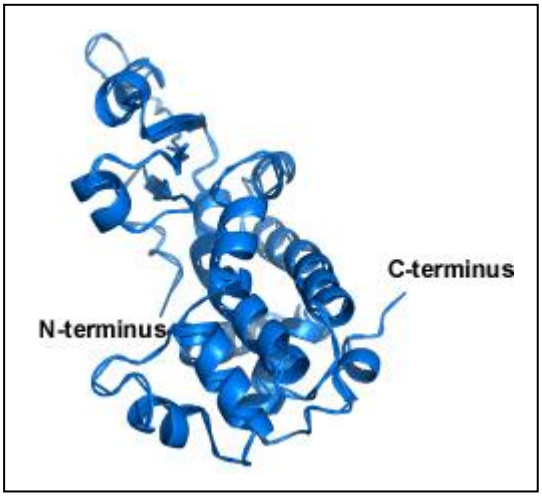

Figure 3-6: Cartoon representation of the crystal structure of yeast GPD1; The C-terminal portion of the structure was solved by molecular replacement using the human enzyme (PDB 1X0V) as probe.

3.2. Saccharopine dehydrogenase1

3.2.1. Construction of pET28b-LYS1

The LYS1 gene (1.1 kb) was provided to me already cloned into pKS by J. Switala. The LYS1-encoding insert was transferred to the expression vector pET28b using the restriction nucleases *Bam*HI and *Nde*I. The restriction pattern of a resulting clone is shown in Fig. 3-7.

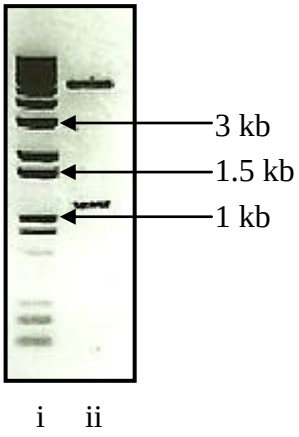

Figure 3-7: Construction of LYS1-pET28b; Lane ii contains the *Bam*HI + *Nde*I restriction digest mixture of DNA from a transformant produced in the ligation of the 1.1 kb fragment into pET28b. The pET28b vector migrates at 5.3 kb and the LYS1 insert at 1.1 kb. Lane i contains the 1 kb DNA ladder.

3.2.2. Protein expression

Small cultures of BL21 cells transformed with pET28b-LYS1 were grown at room temperature, 28 ^{o}C and 37 ^{o}C for induction with 1 mM and 0.1 mM IPTG. LYS1 (41 kDa) expression was better at low IPTG concentration and 28 ^{o}C which was chosen as the optimum temperature (Fig. 3-8).

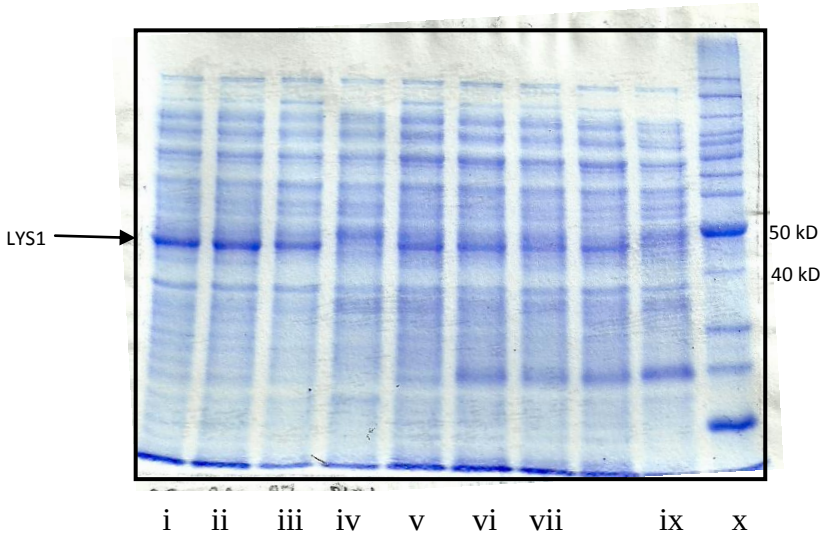

Figure 3-8: Small scale expression trials of LYS1; Lanes i, ii, iii and v, vi, vii contain protein from cultures of pET28b-LYS1 transformed *E. coli* BL21 grown at room temperature, 28 ^{o}C and 37 ^{o}C, respectively. The cultures in lanes i-iii were induced with 0.1 mM IPTG and the cultures in lanes v-vii were induced with 1 mM IPTG. Lanes iv and ix contain protein from a culture of BL21 cells (control). Lane x contains the protein size markers.

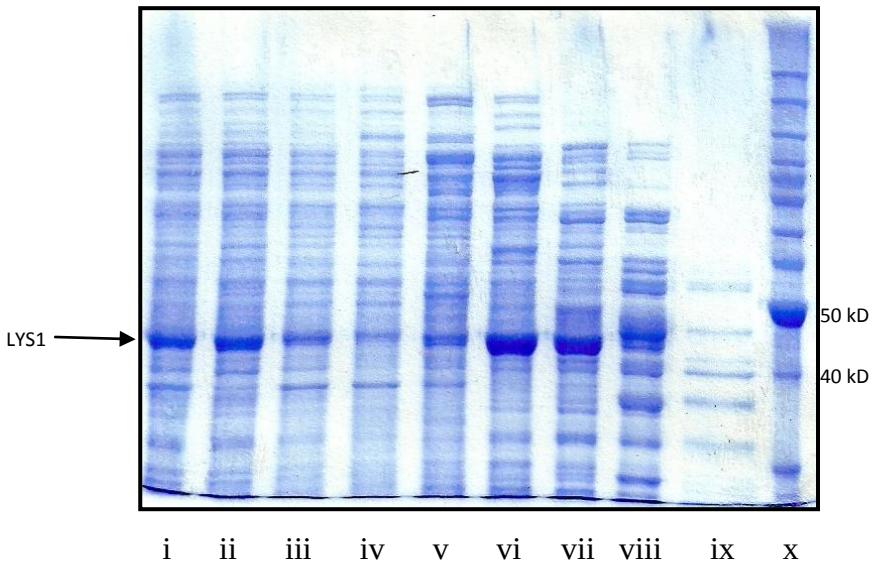

Figure 3-9: Fractionation of LYS1 by ammonium sulfate; Lanes i - ix contain protein fractions from the various stages of LYS1 purification, separated by SDS-PAGE: lane i - crude extract; lane ii - streptomycin sulfate supernatant; lanes iii, iv, v, vi, vii and viii – 20%, 30%, 40%, 50%, 60% and 70% ammonium sulfate pellets respectively; lane ix - 70% ammonium sulfate supernatant. Lane x contains protein size markers.

3.2.3. Protein purification

LYS1 was purified utilizing sequentially, streptomycin sulfate treatment, ammonium sulfate precipitation, ion exchange chromatography on DEAE cellulose and affinity chromatography on a HiTrap nickel column. The results of fractionation by ammonium sulfate are shown in Fig. 3-9.

Ion exchange chromatography

Following ammonium sulfate precipitation, the resuspended pellets from 50% and 60% saturations of ammonium sulfate were loaded on a DEAE Cellufine A500 column as describe in the Methods section and then, equilibrated with 50 mM Tris-HCl pH 7.0. The column was washed thoroughly with 50 mM Tris-HCl pH 7.0, until the absorbance at 280 nm was below 0.025. Subsequently, a linear gradient of 500 mL of 50 mM Tris-HCl pH 8.0 and 500 mL of 0.5 M NaCl in the same buffer was applied. Approximately, 80 drop fractions were collected and analyzed for absorbance at 280 nm (Fig. 3-10, panel A). Fractions were also analyzed by SDS-PAGE and fractions containing the highest concentrations of LYS1 were pooled and concentrated to 10-12 mg/mL. As shown in Fig. 3-10, panel B, the protein was not pure and required further purification.

A

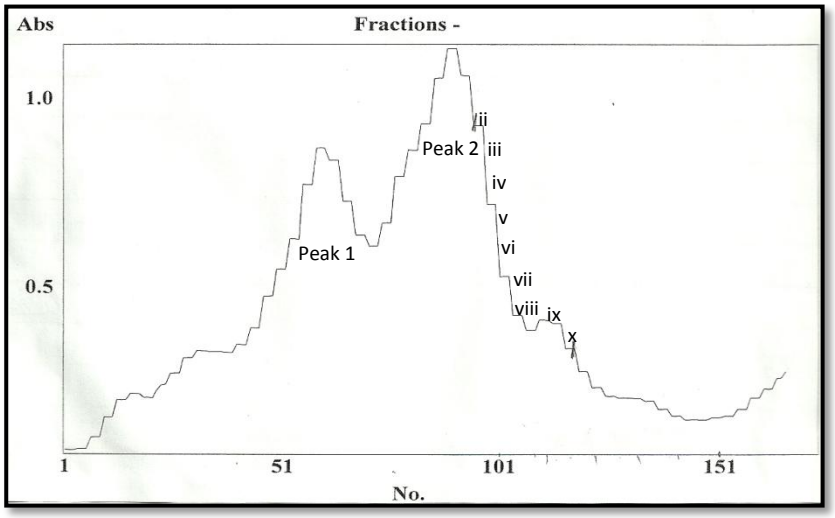

B

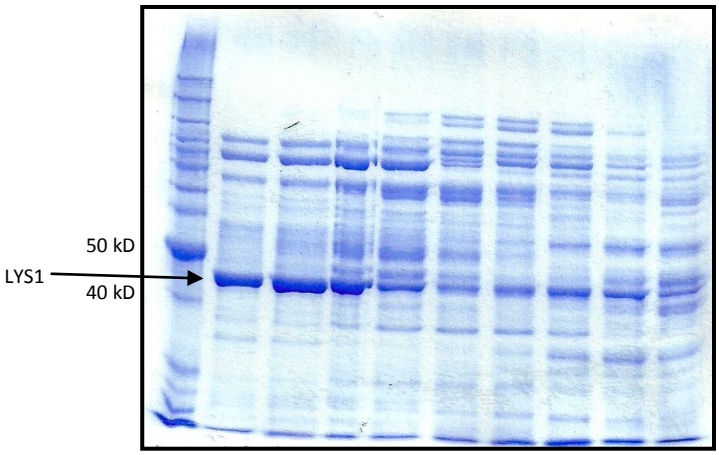

i ii iii iv v vi vii viii ix x

Figure 3-10: Purification of LYS1 on DEAE cellulose; (A) Elution profile of protein assayed at 280 nm. Two peaks of protein eluted and the regions marked by the numbers, ii - x correspond to the fractions containing LYS1. (B) Lanes ii – x contain protein fractions from the elution stage of peak 2, panel A which are separated by SDS-PAGE. Lane i contains protein size markers.

Affinity chromatography

Two types of resins were investigated to improve the purity of LYS1.

(a) 1 mL HiTrap column: After equilibration, the column was loaded with 12 mg of the dialyzed DEAE fraction and washed with 20 column volumes of binding buffer. Protein was eluted by washing successively with 5 mM, 25 mM, 50 mM and 75 mM imidazole. Fractions were analyzed by SDS-PAGE (Fig. 3-11, panel A) and fractions of pure protein were pooled and concentrated to 1-2 mg/mL (Fig. 3-11, panel B). Unfortunately, it was difficult to obtain reproducible results using this type of column and an alternate method was tried.

(b) Ni-NTA Superflow resin: After equilibration, the column was loaded with protein from the 50% and 60% ammonium sulfate precipitations. After washing with 8-10 column volumes of binding buffer, 10 column volumes of 25 mM and then 50 mM imidazole in the same buffer were also applied. Finally, the pure fractions containing LYS1 were eluted with binding buffer containing 250 mM imidazole. The elution profile is shown in figure 3-12, panel A. Fractions were analyzed by SDS-PAGE (Fig. 3-12, panel B) and those containing pure LYS1 were pooled and concentrated to 6-8 mg/mL (Fig. 3-12, panel C). A total of ~20 - 40 mg of protein was dialyzed and frozen as described in section 2.7.2.

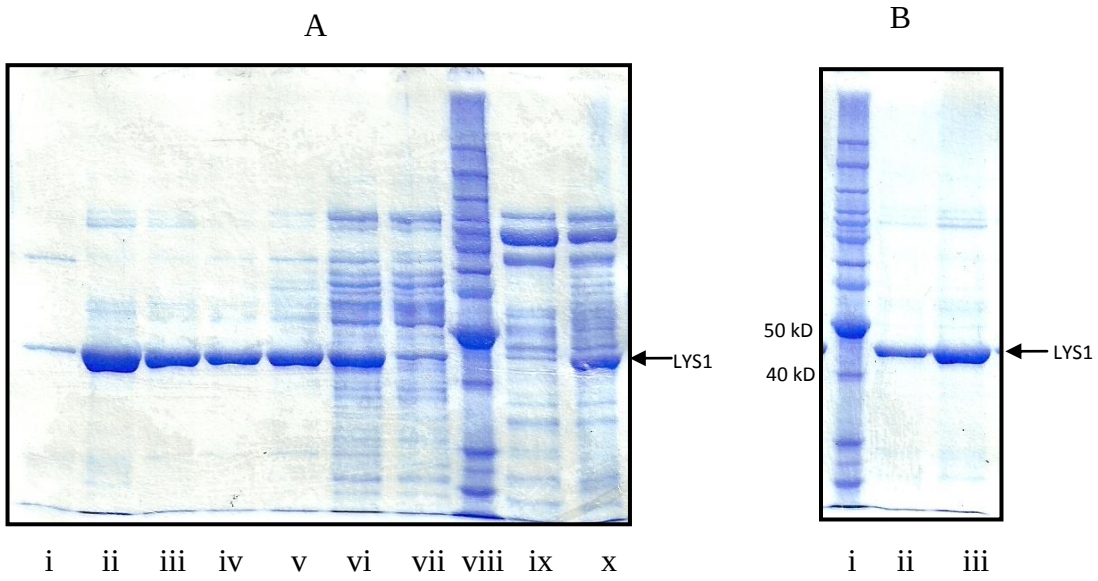

Figure 3-11: Purification of LYS1 on 1 mL HiTrap nickel column; (A) SDS-PAGE showing the fractions eluted at different concentrations of imidazole. Lane i - 75 mM imidazole; lanes ii and iii - 50 mM imidazole; lanes iv, v vi and vii - 25 mM imidazole. Lane viii contains protein size markers. Lane ix contains the fraction eluted in the binding buffer wash and lane x contains the control (concentrated and dialyzed fraction after DEAE). (B) Lanes ii and iii contain 3 and 5 micrograms respectively of concentrated LYS1; lane i contains protein size markers.

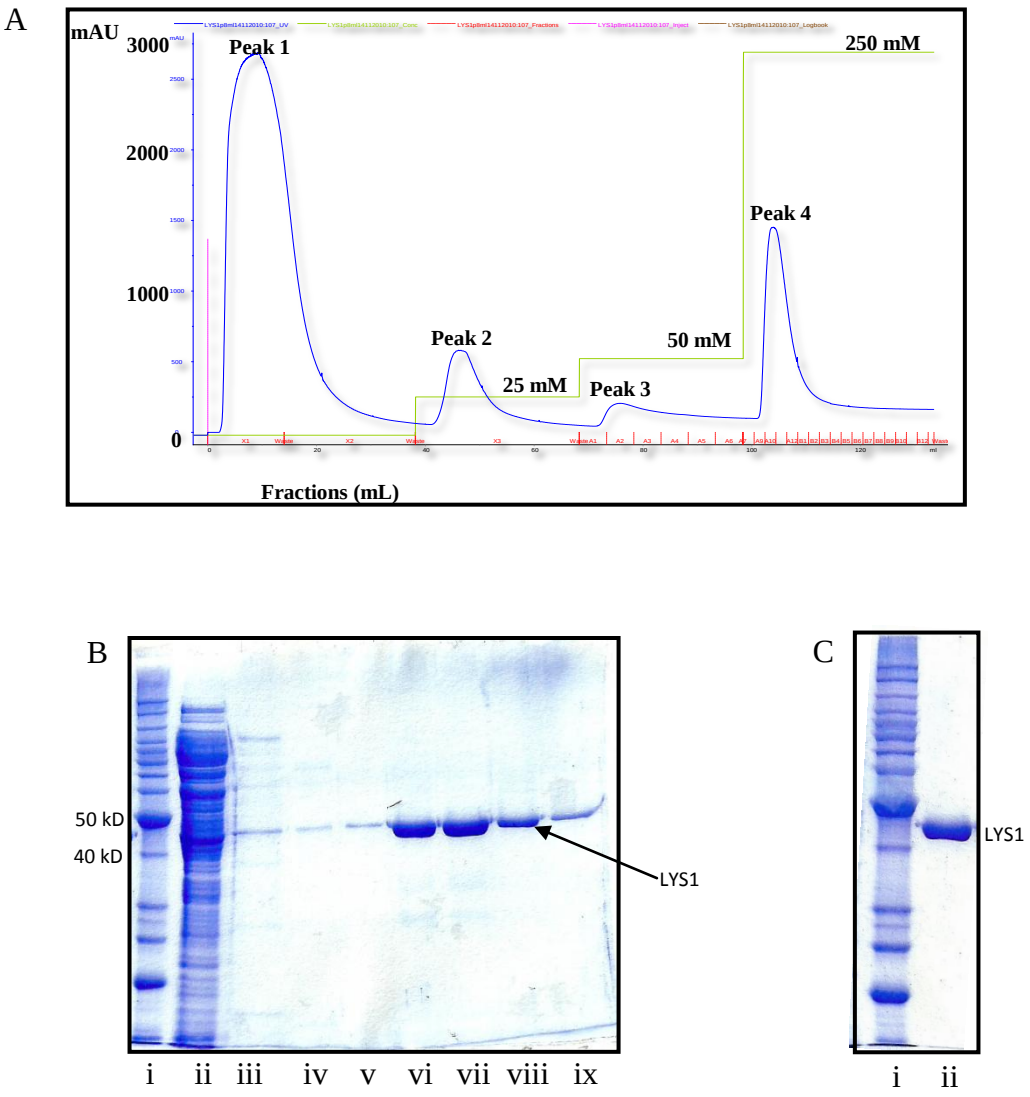

Figure 3-12: Purification of LYS1 on Ni-NTA Superflow resin; (A) Elution profile of protein when ~150 mg of ammonium sulfate saturation was loaded and eluted with step-up gradients of imidazole. Peak i refers to the flow-through; peaks ii, iii, iv refer to the fractions eluted with 25 mM, 50 mM and 250 mM imidazole respectively. (B) Lane i contains protein size markers and lane ii contains the flow-through. Lanes iii, iv, v - ix contain protein eluted with 25 mM, 50 mM and 250 mM imidazole respectively separated by SDS-PAGE. (C) Lane ii contains 3 micrograms of purified LYS1 after separation by SDS-PAGE. Lane i contains protein size markers.

3.2.4. Enzyme activity of LYS1

The saccharopine dehydrogenase activity of LYS1 was determined spectrophotometrically by measuring the decrease in NADH absorbance at 340 nm. A specific activity of 0.01 µmol/min/µg was determined which was almost identical that the activity previously determined (Ogawa and Fujioka, 1977).

3.3. Peroxin7

3.3.1. Construction of pET28b-PEX7

The yeast chromosomal clone of PEX7 used as the starting point for this work was obtained from Open Biosystems. A 1.1 kb DNA fragment resulted from PCR amplification (Fig. 3-13, panel A). Restriction digestion of the cloned plasmid in pKS by *Sst*I and *Xho*I yielded two bands of pKS (3 kb) and *PEX7* (1.1 kb) on agarose gel (Fig. 3-13, panel B). Moreover, digestion of the cloned plasmid in pET28b by same endonucleases yielded the bands of *PEX7* along with pET28b (5.3 kb) (Fig. 3-13, panel C).

3.3.2. Protein expression

Small cultures of BL21 cells expressing PEX7 were grown at room temperature, 28 ^{o}C and 37 ^{o}C and induced with either 0.1 mM or 1 mM IPTG. The expression of PEX7 (42.3 kDa) at high IPTG concentration (Figure 3-14) was found out to be a little better than that at low levels of IPTG and 28 ^{o}C was chosen as the optimum temperature for induction. Several concentrations of glycerol (0.5% - 5%) were added to the culture media in an attempt to enhance the proper folding and expression of PEX7, but there was no appreciable difference in the expression.

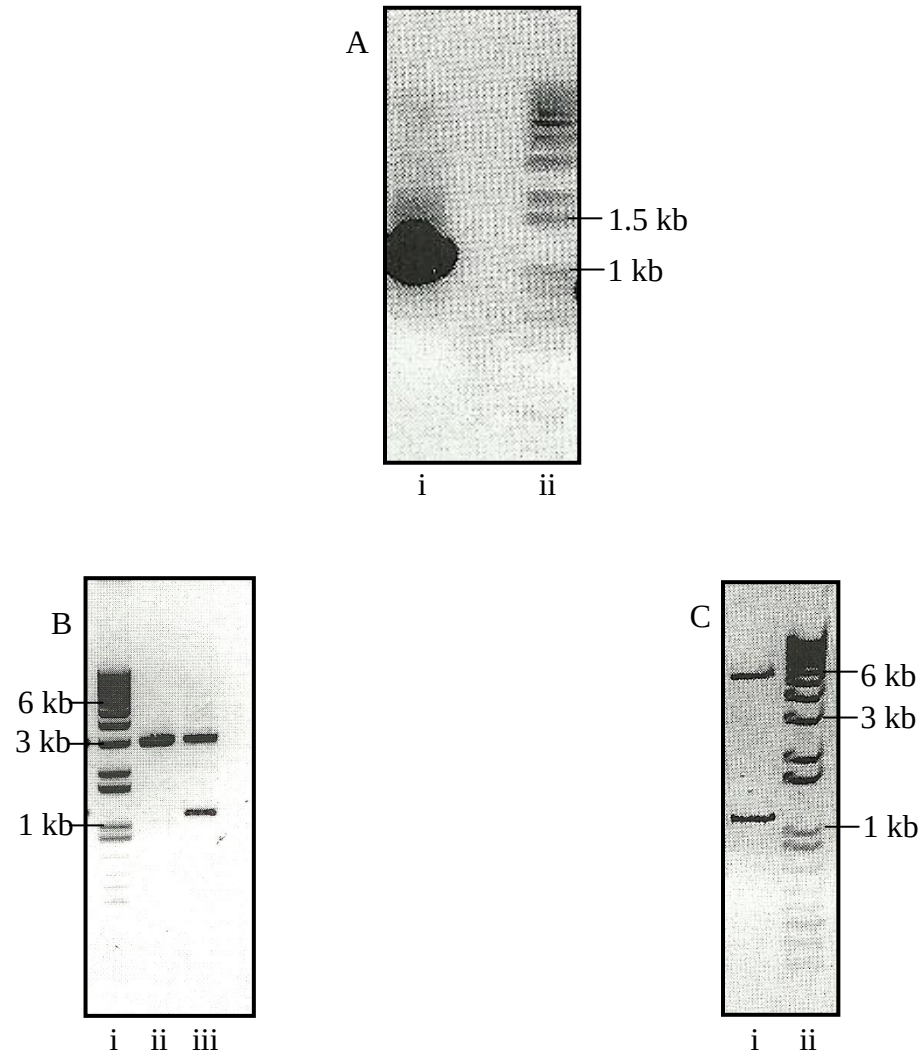

Figure 3-13: Construction of PEX7-pKS and PEX7-pET28b; (A) Lane i contains PCR product containing PEX7 that migrates at 1.1 kb. (B) Lane ii contains pKS DNA and lane iii contains pKS-PEX7 DNA cut with *Sst*I and *Xho*I restriction nucleases. The pKS vector migrates at 2.9 kb and the PEX7 insert migrates at 1.1 kb. (C) Lane i contains pET28b-PEX7 DNA cut with *Sst*I and *XhoI* restriction nucleases. The pET28b vector migrates at 5.3 kb and the PEX7 insert at 1.1 kb. Lanes ii, i, ii of panels (A), (B) and (C) respectively contain 1 kb DNA ladder.

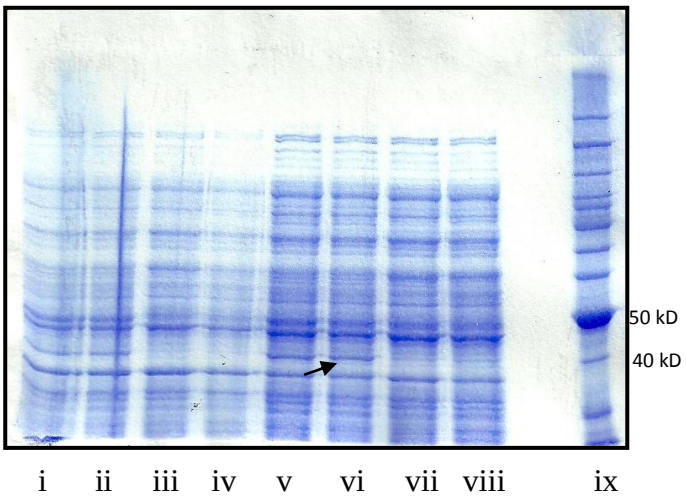

Figure 3-14: Small scale expression trials of PEX7; Lanes i, ii, iii contain debris from cultures of pET28b-PEX7 transformed *E. coli* BL21 grown at room temperature, 28 ^{o}C, 37 ^{o}C respectively and lanes v, vi, vii contain crude extracts from the same grown at room temperature, 28 ^{o}C, 37 ^{o}C respectively, both following 1 mM IPTG induction. Lanes iv and viii contain debris and crude extracts of BL21 cells (control) respectively. Lane ix contains the protein size markers.

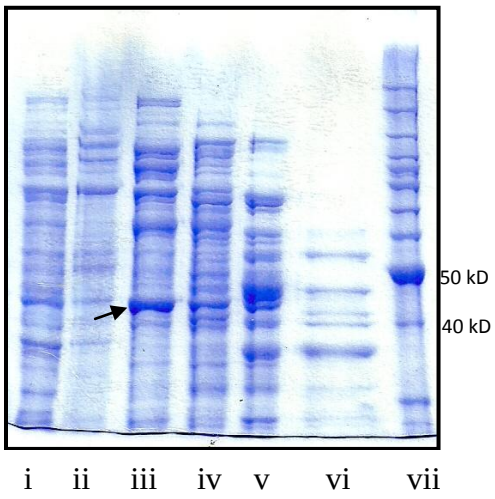

Figure 3-15: Fractionation of PEX7 by ammonium sulfate; Lanes i - vi contain protein fractions from the various stages of PEX7 purification are separated by SDS-PAGE: lane i - crude extract; lanes ii, iii, iv and v - 40%, 50%, 60% and 70% ammonium sulfate pellets; lane vi - 70% ammonium sulfate supernatant. Lane vii contains protein size markers.

3.3.3. Protein purification

Initially, PEX7 was partially purified using a sequence of streptomycin sulfate and ammonium sulfate precipitations. The 50% ammonium sulfate pellet contained the most PEX7 (Fig. 3-15). Subsequently, problems (like, very low concentration of pure protein, tough to eliminate most of the background proteins, nickel column inconsistencies) were encountered necessitating an investigation of several different protocols, like affinity chromatography, size exclusion chromatography and ion exchange chromatography.

Size exclusion chromatography

Following ammonium sulfate precipitation, the 50% and 60% saturations of ammonium sulfate fractions were loaded on a size exclusion column (Superose 12), as described in the section 2.7.3. The elution profile consistently showed two peaks (Figure 3-16, panel A), but analysis of the fractions by SDS-PAGE (Fig. 3-16, panel B) revealed that the protein was not pure.

Affinity chromatography

The fraction from size exclusion chromatography was loaded on a 1 mL HiTrap column (see section 3.2.3). Protein was eluted with 25, 50 and 250 mM imidazole and fractions analyzed by SDS-PAGE revealing relatively pure PEX7 in the 50 mM fraction (Fig. 3-16, panel C). Analysis of the concentrated sample, 0.5 – 1 mg, (Fig. 3-16, panel D) revealed that the protein was not sufficiently pure for crystal trials. Therefore, some other purification methods were needed to be explored.

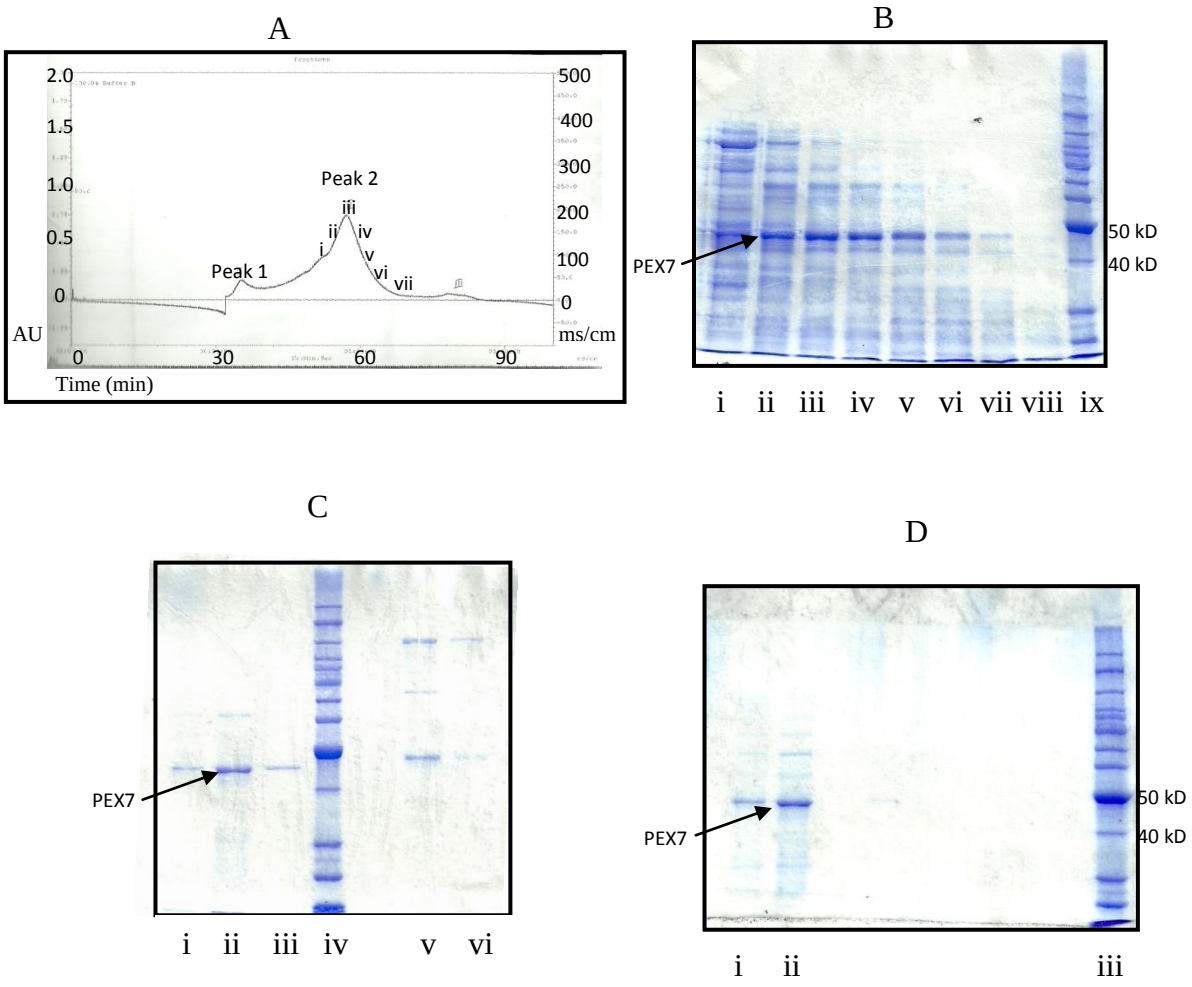

Figure 3-16: Purification of PEX7 on Superose 12 followed by nickel column; (A) Elution profile of 5 mg of protein from 50% and 60% ammonium sulfate saturations, loaded. Two peaks eluted and the region marked by the numbers, i-vii corresponds to the fractions containing PEX7. (B) Lanes i – viii contain protein fractions from the elution stage of peak 2, panel A separated by SDS-PAGE. Lane ix contains protein size markers. (C) Lanes i, ii, iii contain protein eluted with 50 mM imidazole and lanes v, vi contain protein eluted with 25 mM imidazole, separated by SDS-PAGE. Lane iv contains protein size markers. (D) Lanes i and ii contain 3 and 5 µgs respectively of concentrated PEX7; lane iii contains protein size markers.

Ion exchange chromatography

Approximately 500 mg of protein from the 50% and 60% ammonium sulfate pellets was loaded on a DEAE cellulose-cellufine column (see section 3.2.3). The protein fractions were eluted and analyzed at absorbance A_{280} nm (Fig. 3-17, panel A), followed by SDS-PAGE (Figure 3-17, panel B). Fractions containing PEX7 were pooled, concentrated (60 – 70 mg) and then loaded on a nickel column yielding the moderately pure PEX7 (42.3 kDa) shown in (Fig. 3-17, panel C). The final concentration of 1- 1.5 mg/mL (Fig. 3-17, panel D) was too low to proceed with crystallization trials.

Expression in Rosetta (DE3)

To investigate an alternate expression system, Rosetta (DE3) cells expressing PEX7 were grown at room temperature, 28 ^{o}C and 37 ^{o}C with the induction by 1 mM IPTG. While there was some PEX7 in the crude extract supernatant (Fig. 3-18, panel A), the cell debris fraction contained the majority of the protein (Fig. 3-18, panel B) which was found out to be quite unusual, as based on studies, PEX7 is a soluble receptor (Zhang and Lazarow, 1995). The optimum temperature for expression was found to be 28 ^{o}C.

Solubilization and purification of protein from debris

A denaturing protocol was carried out to solubilize the protein from cell debris as described in section 2.7.3. After solubilization (Fig. 3-19, panel A), the protein was loaded on a Ni-NTA Superflow column and eluted with imidazole (Fig. 3-19, panel B). It was promising because protein overexpression was achieved and this might be solubilized with the help of any other denaturing protocol or by using detergents in near future. The protein precipitated during dialysis in refolding buffer and a protein solution useful for crystallization was never obtained.

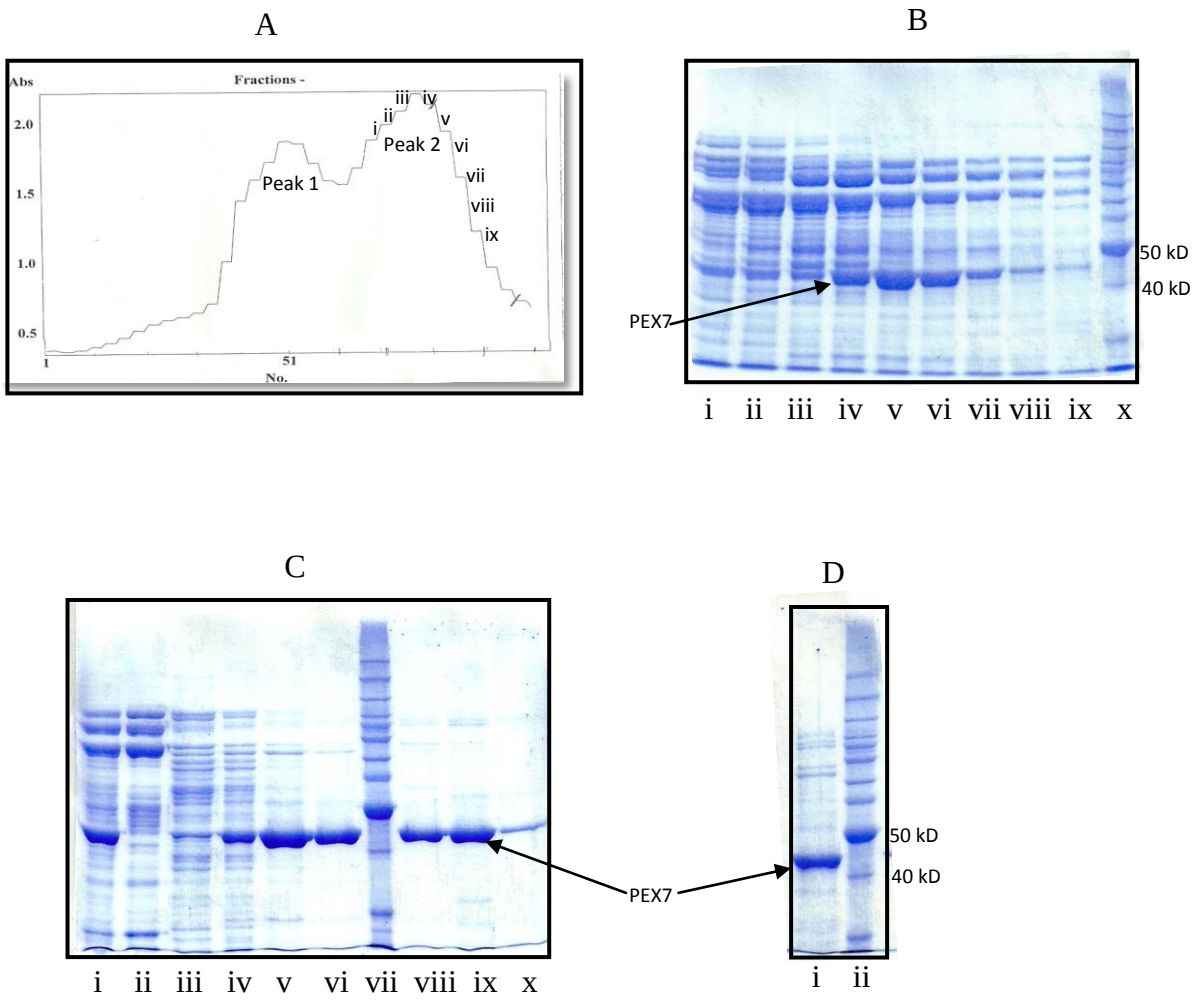

Figure 3-17: Purification of PEX7 on DEAE cellulose followed by nickel column; (A) Elution profile of protein assayed at 280 nm. Two peaks were formed and the region marked by the numbers, i-ix corresponds to the fractions containing PEX7. (B) Lanes i – ix contain protein fractions from the elution stage of peak 2, panel A which are separated by SDS-PAGE. Lane x contains protein size markers. (C) Lane i contains control (concentrated and dialyzed fraction after DEAE) and lane ii contains flow-through. Lanes iii, iv, v, vi contain protein eluted with 25 mM imidazole and lanes viii, ix, x contain protein eluted with 50 mM imidazole, separated by SDS-PAGE. Lane vii contains protein size markers. (D) Lane i contains 5 µg of moderately purified PEX7 after separation by SDS-PAGE. Lane ii contains protein size markers.

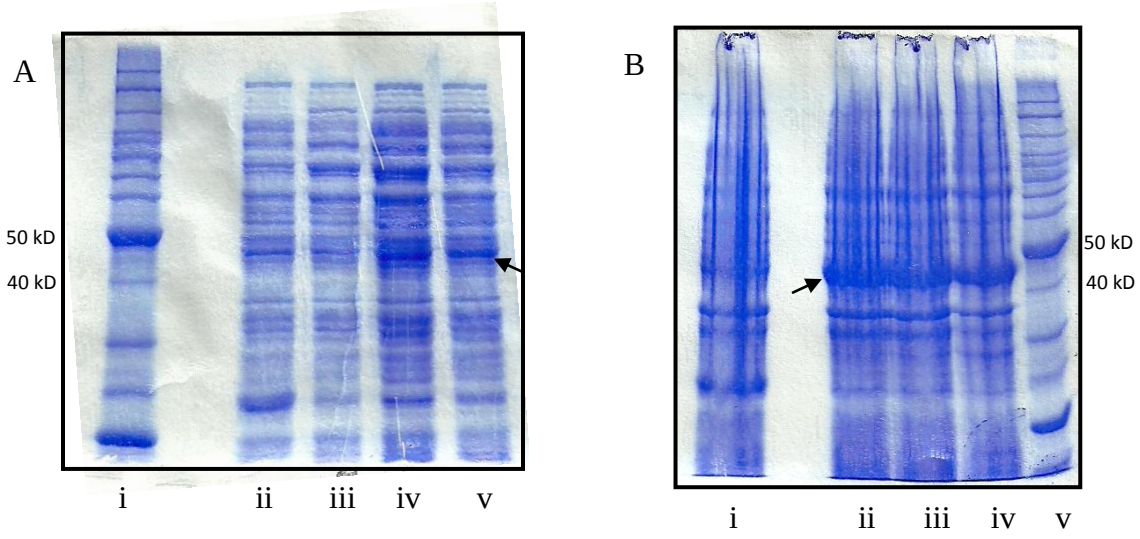

Figure 3-18: Protein expression in Rosetta (DE3); (A) Lane i contains the protein size markers. Lane ii contains soluble protein from the culture of *E. coli* BL21 cells (control). Lanes iii, iv, v contain crude extracts from cultures of pET28b-PEX7 transformed *E. coli* BL21 grown at 37 ^{o}C, 28 ^{o}C and room temperature respectively (42 kDa PEX7 is marked by the arrow), all separated by SDS-PAGE. (B) Lane i contains debris protein from the culture of BL21 cells (control). Lanes ii, iii, iv contain cell debris from cultures of pET28b-PEX7 transformed BL21 grown at room temperature, 28 ^{o}C and 37 ^{o}C respectively (42 kDa PEX7 is marked by an arrow), all separated by SDS-PAGE. Lane v contains the protein size markers.

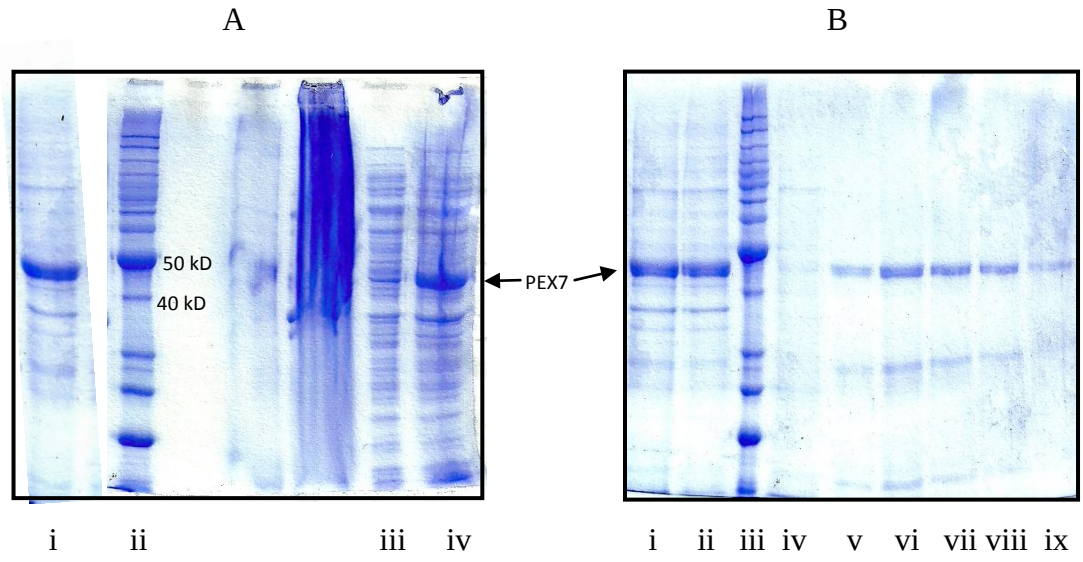

Figure 3-19: Solubilization of cell debris and purification on Ni-NTA Superflow resin; (A) Lane i contains the final supernatant after treating with 6 M guanidine hydrochloride, lane iii contains the crude extract after French Press and centrifugation and lane iv contains the whole cells of PEX7, all separated by SDS-PAGE. Lane ii contains protein size markers. (B) Lane i contains control (soluble protein fraction, same as panel A lane i), lane ii contains flow-through, lane iv contains protein eluted with 25 mM imidazole and lanes v, vi, vii, viii, ix contain protein eluted with 250 mM imidazole, all separated by SDS-PAGE. Lane iii contains protein size markers.

3.4. *In vitro* binding assay

To investigate the interaction between GPD1 and PEX7, an *in vitro* binding assay was performed (see section 2.8). SDS-PAGE (Fig. 3-20) resulted in GPD1 at 42.8 kDa as expected (Albertyn et al., 1994) and PEX7 at 42.3 kDa (Zhang and Lazarow, 1995). Based on a high probability of binding between PTS2-bearing protein – GPD1 and PTS2 receptor – PEX7, co-elution of the two proteins was evident in the result. The mixture was dialyzed and concentrated to 17 mg/mL for use in crystallization trials.

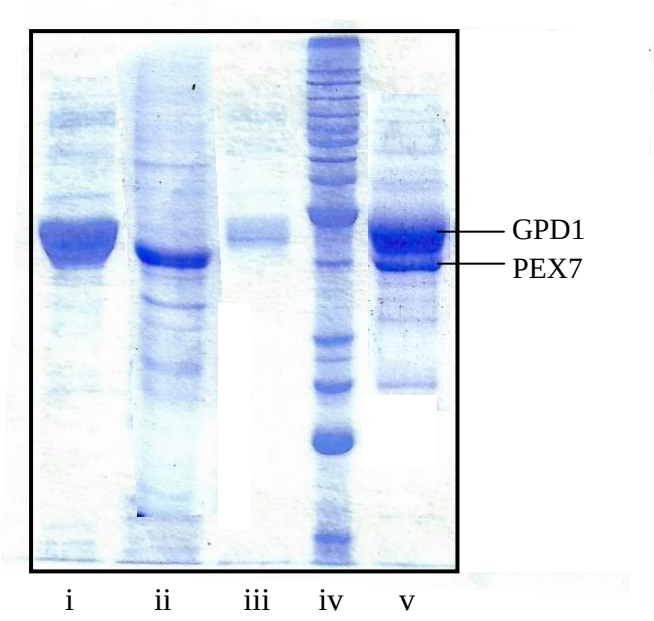

Figure 3-20: *In vitro* binding assay on Ni-NTA Superflow resin; Lanes i and ii contain 5 µg of pure GPD1 and 5 µg of PEX7 (crude extract) respectively; lane iii contains the binding buffer wash. Lane v contains the co-eluted fractions of GPD1+PEX7, loaded 3 µg. Lane iv contains the protein size markers.

4. DISCUSSION

4.1. Expression, purification and crystallization of a subset of *Saccharomyces cerevisiae* peroxisomal proteins

The work described in this thesis is focused on the expression of yeast peroxisomal proteins for the purpose of crystallization and X-ray structure determination. The three proteins studied here were the enzymes GPD1 and LYS1, and the peroxin protein transporter PEX7. Each protein presented a different set of challenges which made trouble shooting various procedures, a major part of the work. Among them, overexpression of recombinant protein using different conditions as well as using different bacterial strains, several purification protocols involving both native and denaturing conditions and techniques related to crystallization.

4.1.1. GPD1

The expression and purification of GPD1 proved to be very straightforward using a protocol involving ion exchange chromatography. This success was followed by a successful crystal screening that led to crystal formation and the collection of diffraction data. A solution for the structure was determined by molecular replacement using the previously determined structure of human GPD1. The C-terminal portion of the protein could be structurally resolved. Several attempts to build the model into the N-terminal 180 residues were made but were not successful. Clearly there was substantial disorder in this portion of the protein but whether this was the result of a limited number of discrete conformations or random disorder is not clear. It was hoped that growing crystals in the presence of substrates such as glycerol phosphate or dihydroxyacetone phosphate might create a more order structure, because the presence of substrate analogue might modulate

the protein's binding sites, thereby resulting in a more ordered and properly folded structure (Xianjin et al., 2006). However, this has not yet been realized so far and work is continuing in this direction.

4.1.2. LYS1

The purification of LYS1 presented more of a challenge with ion exchange chromatography on DEAE cellulose and Hydroxyapatite being unsuccessful. Unlike GPD1 the contaminating proteins could not be fully separated from LYS1. The first attempt to use affinity chromatography using a nickel resin was also unsuccessful when IMAC nickel resin gave inconsistent results. This was eventually attributed to the chelating iminodiacetate on the resin which binds the metal ions at only three ligand sites, providing better binding for the His tag but at the expense of less tightly bound metal ions which leach when strongly chelating proteins are added. Switching to a Ni-NTA resin ultimately provided a reliable and effective purification method. The nitrilotriacetic acid resin chelates the metal ion at four ligand sites which presumably prevents metal leaching.

This is a much easier, one-step purification method resulting in higher yield of pure protein as compared to the purification protocol using glutathione Sepharose where cleavage of GST tag, removal of PreScission protease are pre-requisites to obtain 2.5 mg of pure protein from each litre of cell culture (Burk et al., 2007).

The structure of yeast LYS1 has already been determined begging the question of why it has been targeted for purification. In fact, the structure determination had not been reported when the current work started, and it is very likely that protein may be useful for

binding studies. LYS1 is transported by the PTS1 transporter, PEX5, and the future purification of PEX5 will make possible a study of interactions between the two proteins.

4.1.3. PEX7

PEX7 presented the greatest challenge among the three proteins at both the expression stage and the purification stage. Attempts to improve expression spanned a range of inducer concentrations, media and temperatures with no improvement. Subsequently, the BL21 Tuner cell line which allows for a better control of induction over a broad range of IPTG concentrations was investigated but did not lead to improved expression. Although, the initial purification trials were carried out with the low concentration of PEX7 present in the soluble fractions and that might be one of the causes of getting low concentration of pure protein in the later purification steps.

The possibility that codons rarely used in *E. coli* might be present in the PEX7 clone was investigated by attempting expression in the Rosetta strain which harbours a second plasmid encoding tRNAs that recognize 6 rarely used codons (AUA, AGG, AGA, CUA, CCC and CGA). The expression of PEX7 was greatly improved in this strain, but the protein was predominantly in the cell debris, not the supernatant, suggesting that it had been expressed in inclusion bodies (Rosenberg et al., 1993).

The initial batches of PEX7 which contained low concentrations of the protein in the soluble fraction were subjected to preliminary purification trials which proved to be unsuccessful. The methods tried included size exclusion, ion exchange chromatography and nickel affinity chromatography. In an attempt to improve affinity to the nickel resin, a construct encoding PEX7 with a His tag at both the N- and C-termini was constructed, but also did not lead to any improvement in protein purification.

Ultimately, purification of PEX7 (from debris) was achieved by first denaturing the protein in either 8M urea or 6 M guanidinium hydrochloride and then applying the protein to a Ni-NTA resin. With the His tag fully exposed in the denatured protein, PEX7 exhibited a high affinity for the resin and it eluted as a pure protein. Unfortunately, attempts to renature the protein were unsuccessful with the protein precipitating during dialysis. With large amounts of protein now available, it might be possible to investigate the usefulness of detergents in solubilizing the protein.

The novel method that both solubilized and purified PEX7 (albeit with one other protein present) exploited its property of binding to the PTS2 target protein GPD1. The PEX7-GPD1 complex bound to a Ni-NTA resin and upon elution the PEX7 remained in solution, presumably because it was bound to GPD1. More work is required to achieve the desired 1:1 ratio of the two proteins, but the procedure looks promising both as a means of solubilizing PEX7and in a complex that will be of functional interest.

4.2. Future directions

There are several obvious directions of future work. The complete structure of GPD1 remains to be determined and this might be achieved by the binding of substrates or by exploiting the PEX7-GPD1 complex. The purification of LYS1 makes possible a similar complex formation between PEX5 and LYS1 which could lead to PEX5 purification and to the generation of a functionally important structure to be determined. Once protein structures have been determined, it will be possible to carry out a site directed mutagenesis study to test hypotheses about what features of the proteins are functionally important. Ultimately, this information may lead to a better understanding

of the development and maintenance of peroxisomes in eukaryotic cells and a better understanding of related metabolic diseases.

5. REFERENCES

Agne, B., Meindl, N. M., Niederhoff, K., Einwachter, H., Rehling, P., Sickmann, A., Meyer, H. E., Girzalsky, W. and Kunau, W. H. (2003) Pex8p: an intraperoxisomal organizer of the peroxisomal import machinery. *Molec. Cell.* **11**: 635-46.

Albertini, M., Girzalsky, W., Veenhuis, M., and Kunau, W. H. (2001) Pex12p of *Saccharomyces cerevisiae* is a component of a multi-protein complex essential for peroxisomal matrix protein import. *Eur. J. Cell Biol*. **80**: 257–270.

Alberts, B., Johnson, A., Lewis, J., Raff, M., Roberts, K., and Walter, P. (2002) "Chapter 12: Peroxisomes". *Molecular Biology of the Cell* (Fourth ed.). New York: Garland Science.

Andi, B., West, A. H. and Cook, P. F. (2004) Stabilization and characterization of histidine-tagged homocitrate synthase from *Saccharomyces cerevisiae*. *Arch. Biochem. Biophys*. **421**: 243‑254.

Azevedo, J. E., Costa-Rodrigues, J., Guimarães, C. P., Oliveira, M. E. and Sá-Miranda, C. (2004) Protein translocation across the peroxisomal membrane. *Cell Biochem. Biophys.* **41**: 451-468.

Beopoulos, A., Mrozova, Z., Thevenieau, F., Le Dall, M. T., Hapala, I., Papanikolaou, S., Chardot, T. and Nicaud, J. M. (2008) Control of lipid accumulation in the yeast *Yarrowia lipolytica*. *Appl. Environ. Microbiol.* **74**: 7779–7789.

Berges, D. A., DeWolf, W. E., Jr, Dunn, G. L., Grappel, S. F., Newman, D. J., Taggart, J. J. and Gilvarg, C. (1986) Peptides of 2-aminopimelic acid: antibacterial agents that inhibit diaminopimelic acid biosynthesis. *J. Med. Chem*. **29**: 89‑95.

Bhattacharjee, J. K. (1985) alpha-Aminoadipate pathway for the biosynthesis of lysine in lower eukaryotes. *Crit. Rev. Microbiol*. **12**: 131‑151.

Bhattacharjee, J. K. (1992). Evolution of α-aminoadipate pathway for the synthesis of lysine in fungi. *Evolution of Metabolic Function* (Mortlock, R. P., ed), pp. 47‑80. CRC Press, Boca Raton.

Birschmann, I., Stroobants, A. K., van den Berg, M., Schafer, A., Rosenkranz, K., Kunau, W. H. and Tabak, H. F. (2003) Pex15p of *Saccharomyces cerevisiae* provides a molecular basis for recruitment of the AAA peroxin Pex6p to peroxisomal membranes. *Mol. Biol. Cell* **14**: 2226-36.

Blomberg, A. and Adler, L. (1992) Physiology of osmotolerance in fungi. *Adv. Microb. Physiol.* **33**: 145–212.

Boy-Marcotte, E., Lagniel, G., Perrot, M., Bussereau, F., Boudsocq, A., Jacquet, M. and Labarre, J. (1999) The heat shock response in yeast: differential regulations and contributions of the Msn2p/Msn4p and Hsf1p regulons. *Mol. Microbiol.* **33**: 274–283.

Brauer, M. J., Saldanha, A. J., Dolinski, K. and Botstein, D. (2005) Homeostatic adjustment and metabolic remodeling in glucose-limited yeast cultures. *Mol. Biol. Cell* **16**: 2503–2517.

Braverman, N. G., Steel, C. Obie, Moser, A., Moser, H., Gould, S.J. and Valle, D. (1997) Human *PEX7* encodes the peroxisomal PTS2 receptor and is responsible for rhizomelic chondrodysplasia punctata. *Nat. Genet.* **15**: 369–376.

Brown, L. A. and Baker, A. (2003) Peroxisome biogenesis and the role of protein import. *J. Cell Mol. Med*. **7**: 388-400.

Carvalho, A. F., Pinto, M. P., Grou, C. P., Alencastre, I. S., Fransen, M., Sá-Miranda, C. and Azevedo, J. E. (2007) Ubiquitination of mammalian Pex5p, the peroxisomal import receptor. *J. Biol. Chem.* **282**: 31267-31272.

Cavalier-Smith, T. (1987) The Origin of Eukaryote and Archaebacterial Cells. *Annals of the New York Academy of Science* **503**: 17–54.

Choe, J., Moyersoen, J., Roach, C., Carter, T. L., Fan, E., Michels, PAM and Hol, W. G. J. (2003) Analysis of the sequence motifs responsible for the interactions of peroxins 14 and 5, which are involved in glycosome biogenesis in *Trypanosoma brucei*. *Biochemistry* **42**: 10915-22.

Collins, C. S., Kalish, J. E. and Morrell, J. C. (2000) The peroxisome biogenesis factors Pex4p, Pex22p, Pexlp, and Pex6p act in the terminal steps of peroxisomal matrix protein import. *Mol. Cell Biol*. **20**: 7516-7526.

Costa-Rodrigues, J., Carvalho, A. F., Gouveia, A. M., Fransen, M., Sa-Miranda, C. and Azevedo, J. E. (2004) The N-terminus of the peroxisomal cycling receptor, Pex5p, is required for redirecting the peroxisome-associated peroxin back to the cytosol. *J. Biol. Chem.* **279**: 46573-9.

Dammai, V. and Subramani, S. (2001) The human peroxisomal targeting signal receptor, Pex5p, is translocated into the peroxisomal matrix and recycled to the cytosol. *Cell* **105**: 187-96.

de Duve, C. (1969). The peroxisome: a new cytoplasmic organelle. *Proc. R. Soc. Lond., B. Biol. Sci.* **173**: 71–83.

del Río, L. A., Sandalio, L. M., Palma, J. M., Bueno, P. and Corpas, F. J. (1992) Metabolism of oxygen radicals in peroxisomes and cellular implications. *Free Radic. Biol. Med.* **13**: 557–80.

Distel, B. (1996) An unified nomenclature for peroxisome biogenesis factors. *J. Cell Biol.* **135**: 1-3.

Dodt, G. and Gould, S. J. (1996) Multiple PEX genes are required for proper subcellular distribution and stability of Pex5p, the PTS1 receptor: evidence that PTS1 protein import is mediated by a cycling receptor. *J. Cell Biol.* **135**: 1763–74.

Dodt, G., Braverman, N., Wong, C., Moser, A., Moser, H. W., Watkins, P., Valle, D. and Gould, S. J. (1995) Mutations in the PTS1 receptor gene, PXR1, define complementation group 2 of the peroxisome biogenesis disorders. *Nat. Genet.* **9**: 115-125.

Burk, D. L., Hwang, J., Kwok, E., Marrone, L., Goodfellow, V., Dmitrienko, G. I. and Berghuis, A. M. (2007) Structural studies of the final enzyme in the α-aminoadipate pathway - saccharopine dehydrogenase from *Saccharomyces cerevisiae*. *J. Mol. Biol.* **373**: 745–754.

Eckert, J. H. and Erdmann, R. (2003) Peroxisome biogenesis. *Rev. Physiol. Biochem. Pharmacol.* **147**: 75-121.

Elgersma, Y., Elgersma-Hooisma, M., Wenzel, T., McCaffery, J. M., Farquhar, M. G. and Subramani, S. (1998) A mobile PTS2 receptor for peroxisomal protein import in *Pichia pastoris*. *J. Cell Biol.* **140**: 807–20.

Elgersma, Y., Kwast, L., Klein, A., Voorn-Brouwer, T., Van den Berg, M., Metzig, B., America, T., Tabak, H. F. and Distel, B. (1996) The SH3 domain of the *Saccharomyces cerevisiae* peroxisomal membrane protein Pex13p functions as a docking site for Pex5p, a mobile receptor for the import PTS1-containing proteins. *J. Cell Biol.* **135**: 97–109.

Fujiki, Y. (2000) Peroxisome biogenesis and peroxisome biogenesis disorders. *FEBS Lett.* **476**: 42–46.

Gabaldón, T. (2010) Peroxisome diversity and evolution. *Philos. Trans. R. Soc. Lond. B., Biol. Sci.* **365** (1541): 765–73.

Garrad, R. C. and Bhattacharjee, J. K. (1992) Lysine biosynthesis in selected pathogenic fungi: characterization of lysine auxotrophs and the cloned LYS1 gene of *Candida albicans*. *J. Bacteriol*. **174**: 7379‑7384.

Gatto, G. J. Jr., Geisbrecht, B. V., Gould, S. J. and Berg, J. M. (2000) Peroxisomal targeting signal-1 recognition by the TPR domains of human PEX5. *Nat. Struct. Biol.* **7**: 1091-5.

Geraghty, M. T., Bassett, D., Morrell, J. C., Gatto, G. J., Bai, J. Jr., Geisbrecht, B. V., Hieter, P. and Gould, S. J. (1999) Detecting patterns of protein distribution and gene expression in silico. *Proc. Natl. Acad. Sci.* USA **96**: 2937–2942.

Ghys, K., Fransen, M., Mannaerts, G. P. and Van Veldhoven, P. P. (2002) Functional studies on human Pex7p: subcellular localization and interaction with proteins containing a peroxisome-targeting signal type 2 and other peroxins. *Biochem. J.* **365**: 41–50.

Girzalsky, W., Rehling, P., Stein, K., Kipper, J., Blank, L., Kunau, W. H. and Erdmann, R. (1999) Involvement of Pex13p in Pex14p localization and peroxisomal targeting signal 2-dependent protein import into peroxisomes. *J. Cell Biol.* **144**: 1151–62.

Godon, C., Lagniel, G., Lee, J., Buhler, J. M., Kieffer, S., Perrot, M., Boucherie, H., Toledano, M. B. and Labarre, J. (1998) The H_2O_2 stimulation in *Saccharomyces cerevisiae*. *J. Biol. Chem.* **273**: 22480–22489.

Gould, S. J., Keller, G. A., Hosken, N., Wilkinson, J. and Subramani, S. (1989) A conserved tripeptide sorts proteins to peroxisomes. *J. Cell Biol.* **108**: 1657-1664.

Gouveia, A. M., Guimarães, C. P., Oliveira, M. E., Sá-Miranda, C. and Azevedo, J. E. (2003) Insertion of Pex5p into the peroxisomal membrane is cargo protein dependent. *J. Biol. Chem*. **278**: 4389-4392.

Hohfeld, J., Veenhuis, M. and Kunau, W. H. (1991) PAS3, a *Saccharomyces cerevisiae* gene encoding a peroxisomal integral membrane protein essential for peroxisome biogenesis. *J. Cell Biol.* **114**: 1167–1178.

Jardim, A., Rager, N., Liu, W. and Ullman, B. (2002) Peroxisomal targeting protein 14 (PEX14) from *Leishmania donovani* - molecular, biochemical and immunocytochemical characterization. *Mol. Biochem. Parasitol.* **124**: 51-62.

Kalish, J. E., Keller, G. A., Morrell, J. C., Mihalik, S. J., Smith, B., Cregg, J. M. and Gould, S. J. (1996) A unified nomenclature for peroxisome biogenesis factors. *EMBO J.* **15**: 3275–3285.

Koerkamp, M. G., Rep, M., Bussemaker, H. J., Hardy, G. P., Mul, A., Piekarska, K., Szigyarto, C. A., De Mattos, J. M. and Tabak, H. F. (2002) Dissection of transient oxidative stress response in *Saccharomyces cerevisiae* by using DNA microarrays. *Mol. Biol. Cell* **13**: 2783–2794.

Kunau, W. H., Dommes, V. and Schulz, H. (1995) Beta-oxidation of fatty acids in mitochondria, peroxisomes and bacteria: a century of continued progress. *Prog. Lipid Res.* **34**: 267-342.

Larsson, C., Påhlman, I. L., Ansell, R., Rigoulet, M., Adler, L. and Gustafsson, L. (1998) The importance of the glycerol 3-phosphate shuttle during aerobic growth of *Saccharomyces cerevisiae. Yeast* **14**: 347–357.

Larsson, K., Ansell, R., Eriksson, P. and Adler, L. (1993) A gene encoding sn-glycerol 3-phosphate dehydrogenase (NAD^+) complements an osmosensitive mutant of *Saccharomyces cerevisiae*. *Mol. Microbiol.* **10**: 1101–1111.

Lazarow, P. B. (2003) Peroxisome biogenesis: advances and conundrums. *Curr. Opin. Cell Biol.* **15**: 489-97.

Lejon, S., Thong, S.Y., Murthy, A., Alqarni, S., Murzina, N.V., Blobel, G.A., Laue, E.D. and Mackay, J.P. (2011) Structural basis for rbap48 binding to fog-1. *J.Biol.Chem.* **286**: 1196-1203.

Ma, C., Agrawal, G. and Subramani, S. (2011) The import of peroxisomal matrix proteins. *J. Cell Biol*. **193**: 7-16.

Mager, W. H. and Varela, J. C. S. (1993) Osmostress response of the yeast Saccharomyces. *Mol. Microbiol.* **10**: 253-258.

Marelli, M., Smith, J. J., Jung, S., Yi, E., Nesvizhskii, A. I., Christmas, R. H., Saleem, R. A., Tam, Y. Y., Fagarasanu, A., Goodlett, D. R., Aebersold, R., Rachubinski, R. A. and Aitchison, J. D. (2004) Quantitative mass spectrometry reveals a role for the GTPase Rho1p in actin organization on the peroxisome membrane. *J. Cell Biol.* **167**: 1099–1112.

Martins, A. M., Cordeiro, C. A. and Ponces Freire, A. M. (2001) In situ analysis of methylglyoxal metabolism in *Saccharomyces cerevisiae*. *FEBS Lett.* **499**: 41–44.

Marzioch, M., Erdmann, R., Veenhuis, M. and Kunau, W. H. (1994) PAS7 encodes a novel yeast member of the WD-40 protein family essential for import of 3-oxoacyl-CoA thiolase, a PTS2-containing protein, into peroxisomes. *EMBO J.* **13**: 4908-4918.

Masanori, H., Yasuku, H., Kamran, G. and Yukio, F. (2011) Interaction defect of the medium isoform of PTS1-receptor PEX5p with PTS2-receptor PEX7p abrogates the PTS2 protein import into peroxisomes in mammals; *J. Biochem.* **149**: 203-210.

Matsumoto, N., Tamura, S. and Fujiki, Y. (2003) The pathogenic peroxin Pex26p recruits the Pex1p-Pex6p AAA ATPase complexes to peroxisomes. *Nat. Cell Biol.* **5**: 454-60.

Maynard, E. L., Gatto, G. J. Jr. and Berg, J. M. (2004) Pex5p binding affinities for canonical and noncanonical PTS1 peptides. *Proteins* **55**: 856-61.

McNew, J. A. and Goodman, J. M. (1994) An oligomeric protein is imported into peroxisomes *in vivo*. *J. Cell Biol.* **127**: 1245-1257.

Motley, A. M., Hettema, E. H., Hogenhout, E. M., Brites, P., Asbroek, T., Wijburg, F. A., Baas, F., Heijmans, H. S., Tabak, H. F., Wanders, R. J. A. and Distel, B. (1997) Rhizomelic chondrodysplasia punctata is a peroxisomal protein targeting disease caused by a non-functional PTS2 receptor. *Nat. Genet.* **15**: 377–380.

Moyersoen, J., Michels, P., Krazy, H., Galland, N., Herman, M. and Hannaert, V. (2005) Peroxisomes, glyoxysomes and glycosomes (Review). *Molecular Membrane Biology* **22**: 133-145.

Mukai, S., Ghaedi, K. and Fujiki, Y. (2002) Intracellular localization, function, and dysfunction of the peroxisome-targeting signal type 2 receptor, Pex7p, in mammalian cells. *J. Biol. Chem.* **277**: 9548–9561.

Neuberger, G., Maurer-Stroh, S., Eisenhaber, B., Hartig, A. and Eisenhaber, F. (2003) Motif refinement of the peroxisomal targeting signal 1 and evaluation of taxon-specific differences. *J. Mol. Biol.* **328**: 567-79.

Nishida, H., Nishiyama, M., Kobashi, N., Kosuge, T., Hoshino, T. and Yamane, H. (1999) A prokaryotic gene cluster involved in synthesis of lysine through the amino adipate pathway: a key to the evolution of amino acid biosynthesis. *Genome Res.* **9**: 1175‑1183.

Okumoto, K., Abe, I. and Fujiki, Y. (2000) Molecular anatomy of the peroxin Pex12p: ring finger domain is essential for Pex12p function and interacts with the peroxisome-targeting signal type 1-receptor Pex5p and a ring peroxin, Pex10p. *J. Biol. Chem.* **275**: 25700-10.

Oliveira, M. E., Gouveia, A. M., Pinto, R. A., Sá-Miranda, C. and Azevedo, J. E. (2003) The energetics of Pex5p-mediated peroxisomal protein import. *J. Biol. Chem.* **278**: 39483-39488.

Palmer, D. R., Balogh, H., Ma, G., Zhou, X., Marko, M. and Kaminskyj, S. G. (2004) Synthesis and antifungal properties of compounds which target the alphaaminoadipate pathway. *Pharmazie* **59**: 93‑98.

Panadero, J., Pallotti, C., Rodríguez-Vargas, S., Randez-Gil, F. and Prieto, J. A. (2006) *J. Biol. Chem.* **281**: 4638-4645.

Petriv, O. I., Tang, L., Titorenko, V. I. and Rachubinski, R. A. (2004) A new definition for the consensus sequence of the peroxisome targeting signal type 2. *J. Mol. Biol.* **341**: 119-34.

Pires, J. R., Hong, X. and Brockmann, C. (2003) The ScPcxl3p SH3 domain exposes two distinct binding sites for Pex5p and Pexl4p. *J. Mol. Biol.* **326**: 1427-1435.

Platta, H. W., Grunau, S., Rosenkranz, K., Girzalsky, W. and Erdmann, R. (2005) Functional role of the AAA peroxins in dislocation of the cycling PTS1 receptor back to the cytosol. *Nat. Cell Biol.* **7**: 817-822.

Platta, H. W. and Erdmann, R. (2007) The peroxisomal protein import machinery. *FEBS Lett.* **581**: 2811–2819.

Purdue, P. E. and Lazarow, P. B. (2001) Peroxisome biogenesis. *Annu. Rev. Cell Dev. Biol.* **17**: 701-752.

Purdue, P. E., Yang, X. and Lazarow, P. B. (1998) Pex18p and Pex21p, a novel pair of related peroxins essential for peroxisomal targeting by the PTS2 pathway. *J. Cell. Biol.* **143**: 1859-69.

Purdue, P. E. and Lazarow, P. B. (2001) Pex18p is constitutively degraded during peroxisome biogenesis. *J. Biol. Chem.* **276**: 47684–47689.

Rainer, B., Orzala, S., Michelle, L. H. and Skaidrite, K. K. (2002) Loss of Compartmentalization Causes Misregulation of Lysine Biosynthesis in Peroxisome-Deficient Yeast Cells. *Eukaryotic Cell* **6**: 978–986.

Reguenga, C., Oliveira, M. E. and Gouveia, A. M. (2001) Characterization of the mammalian peroxisomal import machinery: Pex2p, Pex5p, Pcxl2p, and Pexl4p are subunits of the same protein assembly. *J. Biol. Chem.* **276**: 29935-29942.

Rehling, P., Marzioch, M., Niesen, F., Wittke, E., Veenhuis, M. and Kunau, W. H. (1996) The import receptor for the peroxisomal targeting signal 2 (PTS2) in *Saccharomyces cerevisiae* is encoded by the PAS7 gene. *EMBO J.* **15**: 2901–13.

Rep, M., Albertyn, J., Thevelein, J. M., Prior, B. A. and Hohmann, S. (1999) Different signalling pathways contribute to the control of GPD1 gene expression by osmotic stress in *Saccharomyces cerevisiae*. *Microbiology* **145**: 715–727.

Sacksteder, K.A. and Gould, S. J. (2000) The genetics of peroxisome biogenesis. *Annu. Rev. Genet.* **34**: 623–652.

Saidowsky, J., Dodt, G., Kirchberg, K., Wegner, A., Nastainczyk, W., Kunau, W. H. and Schliebs, W. (2001) The di-aromatic pentapeptide repeats of the human peroxisome import receptor PEX5 are separate high affinity binding sites for the peroxisomal membrane protein PEX14. *J. Biol. Chem.* **276**: 34524-9.

Schrader, M. and Fahimi, H. D. (2006) Growth and division of peroxisomes. *Int. Rev. Cytol.* **255**: 237-290.

Smith, T. F., Gaitatzes, C., Saxena, K. and Neer, E. J. (1999) The WD repeat: a common architecture for diverse functions. *Trends Biochem. Sci.* **24**: 181–5.

Smith, T. F. and Waterman, M. S. (1981) Identification of Common Molecular Subsequences. *J. Mol. Biol* **147**: 195–197.

Snyder, W. B., Koller, A., Choy, A. J., Johnson, M. A., Cregg, J. M., Rangell, L., Keller, G. A. and Subramani, S. (1999) Pex17p is required for import of both peroxisome membrane and lumenal proteins and interacts with Pex19p and the peroxisome targeting signal-receptor docking complex in *Pichia pastoris*. *Mol. Biol. Cell.* **10**: 4005–19.

Stein, K., Schell-Steven, A., Erdmann, R. and Rottensteiner, H. (2002) Interactions of Pex7p and Pex18p/Pex21p with the peroxisomal docking machinery: implications for the first steps in PTS2 protein import. *Mol. Cell. Biol.* **22**: 6056-69.

Subramani, S., Koller, A. and Snyder, W. B. (2000) Import of peroxisomal matrix and membrane proteins. *Annu. Rev. Biochem.* **69**: 399–418.

Sunhee, J., Marcello, M., Rachubinski, R. A., Goodlett, D. R. and Aitchison, J. D. (2010) Dynamic Changes in the Subcellular Distribution of Gpd1p in Response to Cell Stress. *J. Biol. Chem.* **285**: 6739–6749.

Tabak, H. F., Murk, J. L., Braakman, I. and Geuze, H. J. (2003) Peroxisomes start their life in the endoplasmic reticulum. *Traffic* **4**: 512-8.

Titorenko, V. I. and Rachubinski, R. A. (2001) The life cycle of the peroxisome. *Nat. Rev. Mol. Cell. Biol.* **2**: 357-68.

Valadi, A., Granath, K., Gustafsson, L. and Adler, L. (2004) Identification of a cytosolically directed NADH dehydrogenase in mitochondria of *Saccharomyces cerevisiae*. *J. Biol. Chem.* **279**: 39677–39685.

Van den Brink, D. M., Brites, P., Haasjes, J., Wierzbicki, A. S., Mitchell, J., Lambert-Hamill, M., de Belleroche, J., Jansen, G. A., Waterham, H. R. and Wanders, R. J. (2003) Identification of PEX7 as the second gene involved in Refsum disease. *Am. J. Hum. Genet.* **72**: 471–477.

Vladimir and Richard. (2001) The Life Cycle of the Peroxisome. *Nature Reviews, Molecular Cell Biology* **2**: 357-368.

Wanders, R. J. and Waterham, H. R. (2006) Biochemistry of mammalian peroxisomes revisited. *Annu. Rev. Biochem.* **75**: 295–332.

Williams, C., van den Berg, M., Sprenger, R. R. and Distel, B. (2007) A conserved cysteine is essential for Pex4p-dependent ubiquitination of the peroxisomal import receptor Pex5p. *J. Biol. Chem.* **282**: 22534-22543.

Ou1, X., Ji, C., Han, X., Zhao, X., Li1, X., Wong, Y., Bartlam, M. and Rao, Z. (2006) Crystal Structures of Human Glycerol 3-phosphate Dehydrogenase 1 (GPD1) *J. Mol. Biol.* **357**: 858–869.

Xu, H., Andi, B., Qian, J., West, A. H. and Cook, P. F. (2006) The alpha-aminoadipate pathway for lysine biosynthesis in fungi. *Cell Biochem. Biophys*. **46**: 43‑64.

Zabriskie, T. M. and Jackson, M. D. (2000) Lysine biosynthesis and metabolism in fungi. *Nature Prod. Rep.* **17**: 85‑97.

Zhang, J. W. and Lazarow, P. B. (1995) PEB1 (PAS7) in *Saccharomyces cerevisiae* encodes a hydrophilic, intra-peroxisomal protein that is a member of the WD repeat family and is essential for the import of thiolase into peroxisomes. *J. Cell Biol.* **129**: 65-80.

Zinser, E. and Daum, G. (1995) Isolation and biochemical characterization of organelles from the yeast *S. cerevisiae*. *Yeast* **11:** 493-536.